ENVISAT GOMOS Monthly report: November 2003

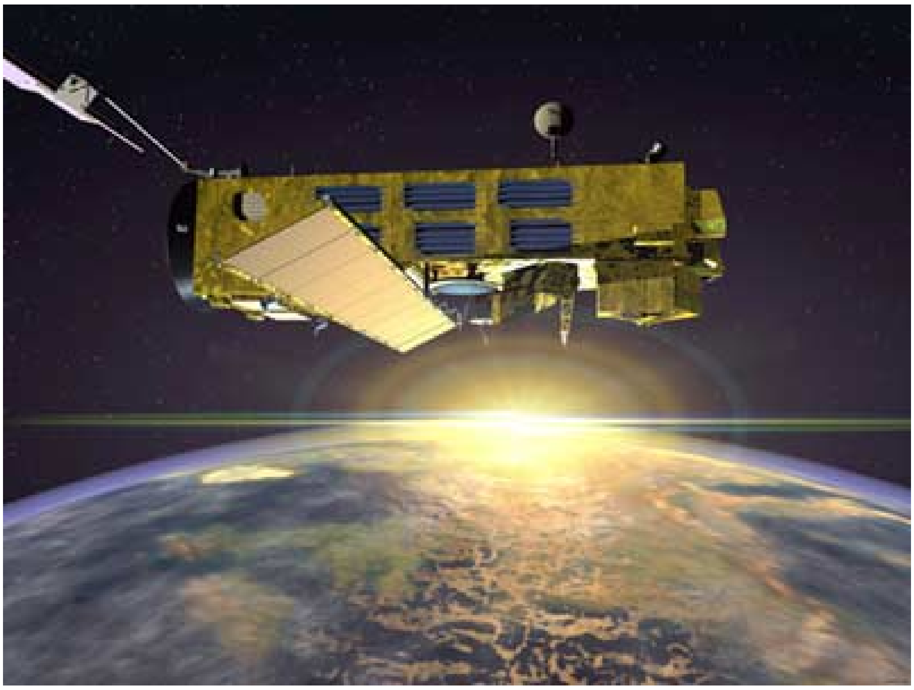

Prepared by:	PCF team	ESA EOP-GOQ
Inputs from:	GOMOS Quality Working Group	
Issue:	1.0	
Reference:	ENVI-SPPA-EOPG-TN-03-0034	
Date of issue:	17 Dec. 03	
Status:	Reviewed	
Document type:	Technical Note	
Approved by:	Pascal Lecomte, Rob Koopman	

TABLE OF CONTENTS

1 INTRODUCTION ... 2
1.1 Scope ... 2
1.2 References ... 2
1.3 Acronyms and abbreviations ... 3

2 SUMMARY ... 4

3 INSTRUMENT UNAVAILABILITY ... 5
3.1 GOMOS unavailability periods ... 5
3.2 Stars lost in centering ... 6
3.3 Data generation gaps ... 8
3.3.1 GOM_NL__0P ... 8
3.3.2 Higher-level products ... 9

4 INSTRUMENT CONFIGURATION AND PERFORMANCE ... 9
4.1 Instrument Operation and Configuration ... 9
4.2 Thermal Performance ... 10
4.3 Optomechanical Performance ... 14
4.4 Electronic Performance ... 15
4.4.1 Dark Charge evolution and trend ... 15
4.4.2 Signal modulation ... 18
4.4.3 Electronic Chain Gain and Offset ... 18
4.5 Acquisition, Detection and Pointing Performance ... 20
4.5.1 SATU noise and equivalent angle ... 20
4.5.2 Tracking loss information ... 21
4.5.3 MIP (Most Illuminated Pixel) ... 24

5 LEVEL 1 PRODUCT QUALITY MONITORING ... 25
5.1 Processor Configuration ... 25
5.1.1 Version ... 25
5.1.2 Auxiliary Data Files (ADF) ... 27
5.2 Quality Flags monitoring ... 29
5.3 Spectral Performance ... 30
5.4 Radiometric Performance ... 31
5.4.1 Radiometric sensitivity ... 31
5.4.2 Pixel Response Non Uniformity (PRNU) ... 34
5.5 Other Calibration Results ... 34

6 LEVEL 2 PRODUCT QUALITY MONITORING ... 34
6.1 Processor Configuration ... 34
6.1.1 Version ... 34
6.1.2 Auxiliary data files (ADF) ... 35
6.2 Other Level 2 performance issues ... 36

7 VALIDATION ACTIVITIES AND RESULTS ... 37
7.1 Intercomparison with external data ... 37
7.2 GOMOS-Climatology comparisons ... 41

7.3 GOMOS Assimilation.. 41
7.4 Consistency Verification: GOMOS-GOMOS intercomparison 43

1 INTRODUCTION

The GOMOS monthly report documents the current status and recent changes to the GOMOS instrument, its data processing chain, and its data products.
The Monthly Report (hereafter MR) is composed of analysis results obtained by the Product Control Facility, combined with inputs received from the different entities working on GOMOS operation, calibration, product validation and data quality. These teams participate in the GOMOS Quality Working Group:

- European Space Agency (ESRIN-PCF, ESOC, ESTEC-PLSO)
- ACRI
- Service d'Aeronomie
- Finnish Meteorological Institute
- IASB-Belgian Institute for Space Aeronomy
- Atrium Space
- ECMWF

In addition, the group interfaces with the Atmospheric Chemistry Validation Team.

1.1 Scope

The main objective of the Monthly Report is to give, on a regular basis, the status of GOMOS instrument performance, data acquisition, results of anomaly investigations, calibration activities and validation campaigns. The following six sections compose the MR:

- Summary
- Unavailability
- Instrument Performance and Configuration
- Level 1 Product Quality Monitoring
- Level 2 Product Quality Monitoring
- Validation Activities and Results

1.2 References

[1] ENVISAT Weekly Mission Operations Report #76, #77, #78, #79 ENVI-ESOC-OPS-RP-1011-TOS-OF
[2] 'Level 1b Detailed Processing Model', PO-RS-ACR-GS-0001, issue 5.4, 20 Nov, 2002
[3] 'Level 2 Detailed Processing Model', PO-RS-ACR-GS-0002, issue 5.4, 20 Nov, 2002

1.3 Acronyms and abbreviations

ACVT	Atmospheric Chemistry Validation Team
ADF	Auxiliary Data File
ADS	Auxiliary Data Server
ANX	Ascending Node Crossing
ARF	Archiving Facility (PDS)
CCU	Central Communication Unit
CFS	CCU Flight Software
CNES	Centre National d'Études Spatiales
CTI	Configuration Table Interface / Configurable Transfer Item
CR	Cyclic Report
DC	Dark Charge
DMOP	Detailed Mission Operation Plan
DPM	Detailed Processing Model
DS	Data Server
DSA	Dark Sky Area
DSD	Data Set Descriptor
ECMWF	European Centre for Medium Weather Forecast
EQSOL	Equipment Switch Off Line
ESA	European Space Agency
ESL	Expert Support Laboratory
ESRIN	European Space Research Institute
ESTEC	European Space Research & Technology Centre
ESOC	European Space Operations Centre
FCM	Fine Control Mode
FMI	Finnish Meteorological Institute
FOCC	Flight Operations Control Centre (ENVISAT)
FP1	Fast Photometer 1
FP2	Fast Photometer 2
GADS	Global Annotations Data Set
GOMOS	Global Ozone Monitoring by Occultation of Stars
GOPR	GOmos PRototype
GS	Ground Segment
HK	Housekeeping
IASB	Institut d'Aeronomie Spatiale de Belgique
IAT	Interactive Analysis Tool
ICU	Instrument Control Unit
IDL	Interactive Data Language
IECF	Instrument Engineering and Calibration Facilities
IMK	Institute of Meteorology Karlsruhe (Meteorologisch Institut Karlsuhe)
INV	Inventory Facilities (PDS)
IPF	Instrument Processing Facilities (PDS)
JPL	Jet Propulsion Laboratory
LAN	Local Area Network
LPCE	Laboratoire de Physique et Chimie de l'Environnement
LUT	Look Up Table
MCMD	Macro Command

MDE	Mechanism Drive Electronics
MIP	Most Illuminated Pixel
MPH	Main Product Header
MPS	Mission Planning System
MR	Monthly Report
OBT	On Board Time
OCM	Orbit Control Manoeuvre
OOP	Out-of-plane
OP	Operational Phase of ENVISAT
PAC	Processing and Archiving Centre (PDS)
PCF	Product Control Facility
PDCC	Payload Data Control Centre (PDS)
PDHS	Payload Data Handling Station (PDS)
PDHS-E	Payload Data Handling Station – ESRIN
PDHS-K	Payload Data Handling Station – Kiruna
PDS	Payload Data Segment
PLSOL	Payload Switch off Line
PMC	Payload Module Computer
PRNU	Pixel Response Non Uniformity
QC	Quality Control
QUARC	Quality Analysis and Reporting Computer
QWG	Quality Working Group
RIVM	Rijksinstituut voor Volksgezondheid en Milieu
RTS	Random Telegraphic Signal
SA	Service d'Aeronomie
SATU	Star Acquisition and Tracking Unit
SFA	Steering Front Assembly
SFCM	Stellar Fine Control Mode
SFM	Steering Front Mechanism
SMNA	Servicio Meteorológico Nacional de Argentina
SODAP	Switch On and Data Acquisition Phase
SPA1	Spectrometer A CCD 1
SPA2	Spectrometer A CCD 2
SPB1	Spectrometer B CCD 1
SPB2	Spectrometer B CCD 2
SPH	Specific Product Header
SQADS	Summary Quality Annotation Data Set
SSP	Sun Shade Position
SZA	Solar Zenith Angle

2 SUMMARY

The GOMOS instrument has been operating nominally during the reporting month. Due to some planned manoeuvres GOMOS was unavailable from 5 Nov 2003 22:08 to 6 Nov 2003 02:50 and from 18 Nov 2003 21:52 to 19 Nov 2003 01:07 (section 3.1).

The availability of level 1b data within the archives is very stable around 98% during the whole month of November. Also the level 0 availability is stable being the percentage situated almost at 100% (section 3.3).

The detector temperatures during November are slightly higher than the ones registered in October and about one degree higher than November 2002. The expected seasonal variation of the temperatures with amplitude of around one degree can be clearly observed (section 4.2).

A new band setting calibration has been performed during November with results that confirm the values of the last calibration analysis done in August (section 4.3).

The elevation at which stars first appear on the star-tracking detector shows some deviations in elevation from the expected position. Stars now initially appear above the SATU elevation centre. The variation in this MIP positions displays seasonal variation and is an indicator of an ENVISAT platform attitude deviation (section 4.5.3).

The variation of the radiometric sensitivity ratio is outside the threshold for some photometer ratios and for some stars. ACRI ESL has performed some investigations (still on going) and two possible causes have been identified up to now: the vignetting correction and an inaccurate reflectivity correction LUT. Future monthly reports will include the latest news on this issue (section 5.4.1).

In this MR the whole set of ADF that have been used by the PDS since the beginning of the mission is reported. Furthermore, on 10th, 17th and 24th November new calibration ADF's were disseminated with only updated DC map of orbits 08852, 08941 and 09050 respectively (section 5.1-2).

ESA has continued the supply of selected data products to validation teams using the prototype processor at ACRI. An upgrade of the data processing algorithm specification is in progress, in order to improve both level 1 and level 2 products.

3 INSTRUMENT UNAVAILABILITY

3.1 GOMOS unavailability periods

In table 3.1-1 there is a list of GOMOS unavailability reports issued during the period 1st November (00:00:00) 2003 until 30th November (24:00:00) 2003. No anomalies occurred to GOMOS during November being the two unavailabilities related to Orbit Control Manoeuvres and hence, planned. The first planned manoeuvre (SFCM) was cancelled due to the on-going uncertainty in solar activity and resulting atmospheric drag predictions. Unfortunately, due to the required 3 day in advance in the planning of GOMOS and the fact that the MPS schedule was already up-linked, it was not possible to bring GOMOS back into nominal operations for that period.

Table 3.1-1 List of unavailability reports issued during November

Reference of unavailability report	Start time Star orbit	Stop time Stop orbit	Description
EN-UNA-2003/0329	5 Nov 2003 22:08:00.000 Day of Year = 309 Orbit = 08801 Anx Offset = 0677.063	6 Nov 2003 02:50:00.000 Day of Year = 310 Orbit = 08803 Anx Offset = 5525.207	Planned: GOMOS unavailable due to FCM. GOMOS was commanded to Heater mode with MDE off and then back to an operational state (PAUSE with SFA calibrated)
EN-UNA-2003/0339	18 Nov 2003 21:52:00.000 Day of Year = 322 Orbit = 08987 Anx Offset = 0234.455	19 Nov 2003 01:07:00.000 Day of Year = 323 Orbit = 08988 Anx Offset = 5898.527	Planned: GOMOS unavailable due to FCM. GOMOS was commanded to Heater mode with MDE off and then back to an operational state (PAUSE with SFA calibrated)

3.2 Stars lost in centering

The acquisition of a star initiates with a rallying phase where the telescope mechanism is directed towards the expected position of the star. Subsequently the acquisition procedure enters into detection mode, where the SATU star tracker output signal is pre-processed for spot presence survey and for the location of the most illuminated couple of adjacent pixels for two added lines, over the detection field. The Most Illuminated Pixel (MIP) defines the position of the first SATU centering window. The next step in the acquisition sequence is then initiated and consists of a centering phase where the SATU output signal is pre-processed for spot presence survey over the maximum of 10x10 pixel field. This allows the third phase to begin: the tracking phase.
The centering phase has occasionally resulted in loss of the star from the field of view. The fig. 3.2-1 reports the percentage of the stars lost in centering for the period 03-FEB-2003 to 30-NOV-2003. It can be seen that some stars, mainly weak stars (higher star id means higher magnitude) are lost during centering phase in more than 4% of their planned observations. As the monitoring shows neither trend nor excessively high percentages of loss, there is no need for the moment to reject any star from the catalogue, and there is no indication of instrument-related problems.

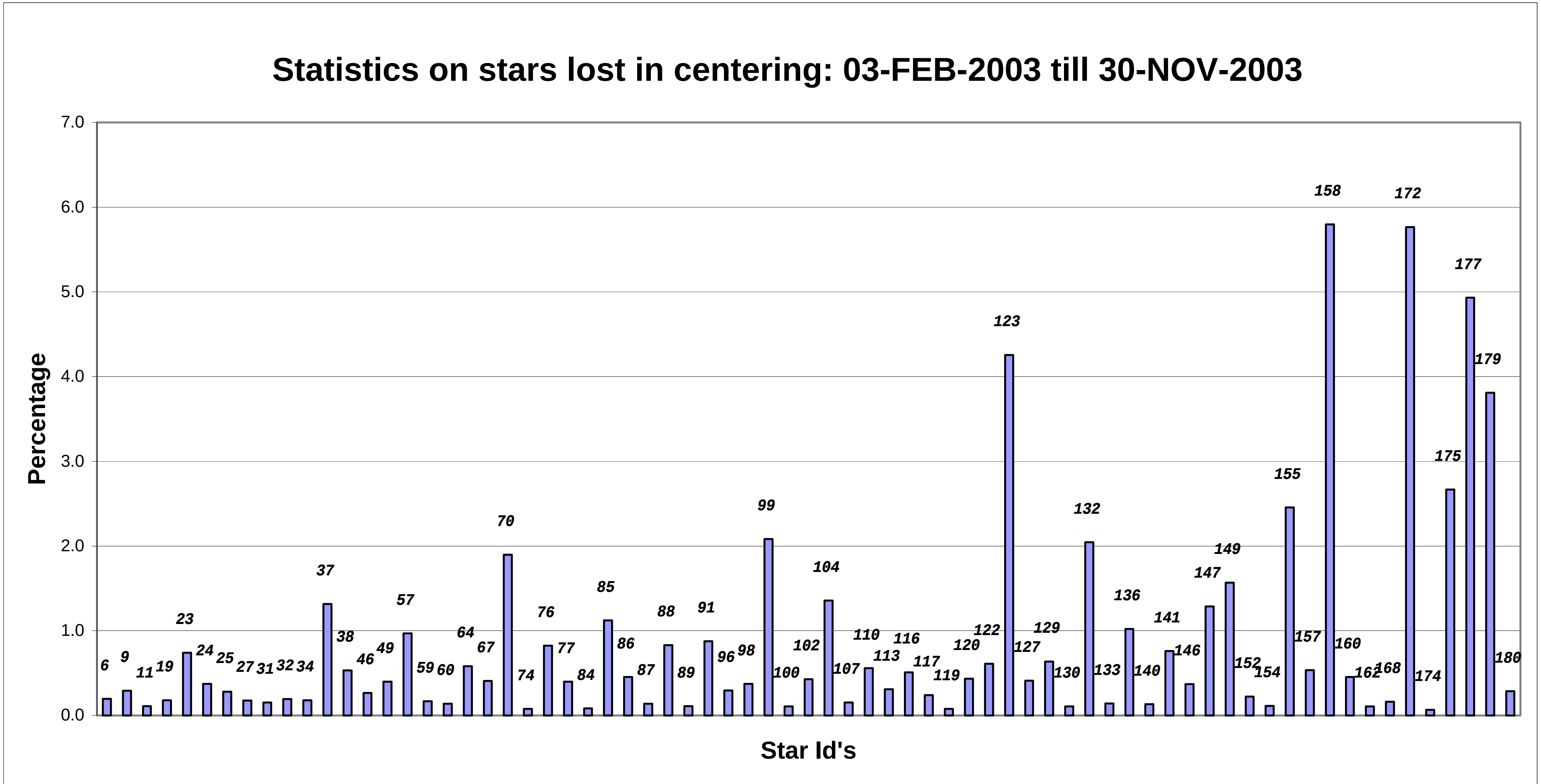

Figure 3.2-1: Statistics on stars that have been lost during the centering phase. The numbers above the columns correspond to the Star Id's.

3.3 Data generation gaps

The trend in percentage of available data within the archives PDHS-K and PDH-E is depicted in fig. 3.3-1 (when instrument was in operation). It is a good indicator on how the PDS chain is working in terms of generation and dissemination of data to the archives. The percentage is calculated once per week.

The availability of level 1b data within the archives is very stable around 98% during the whole month of November. Also the level 0 availability is stable being the percentage situated almost at 100%.

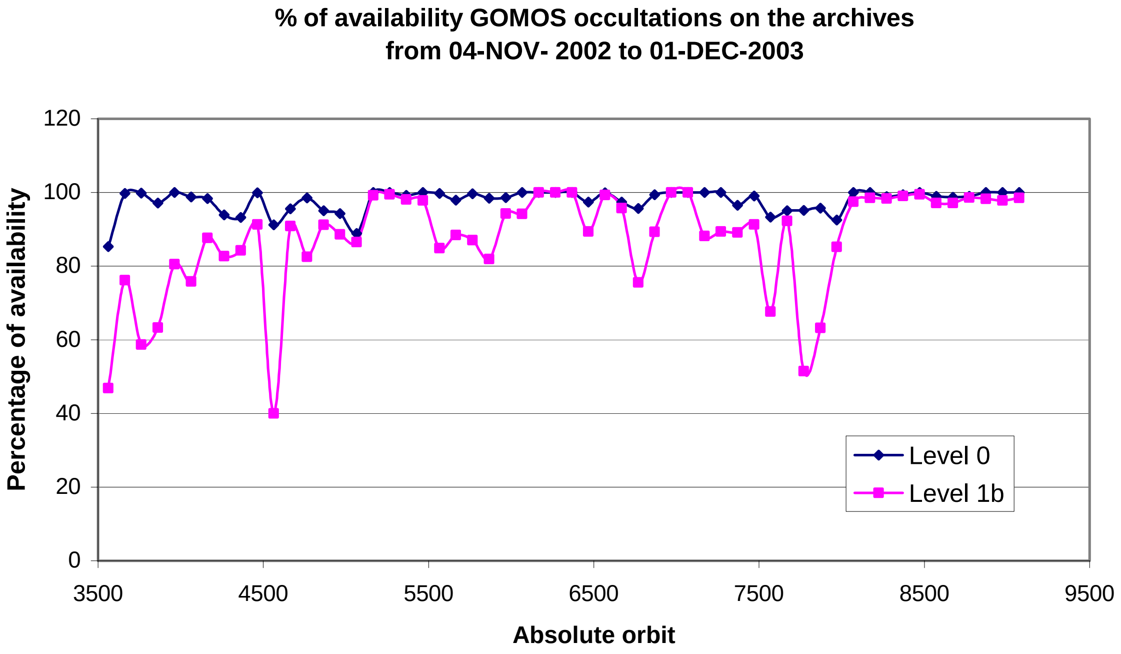

Figure 3.3-1: Percentage of level 0 and level 1b data availability on the archives PDHS-E and PDHS-K

3.3.1 GOM_NL__0P

Occultations planned to be acquired but for which no GOM_NL__0P data product has become available are presented in fig. 3.3-2 for the month of November 2003.

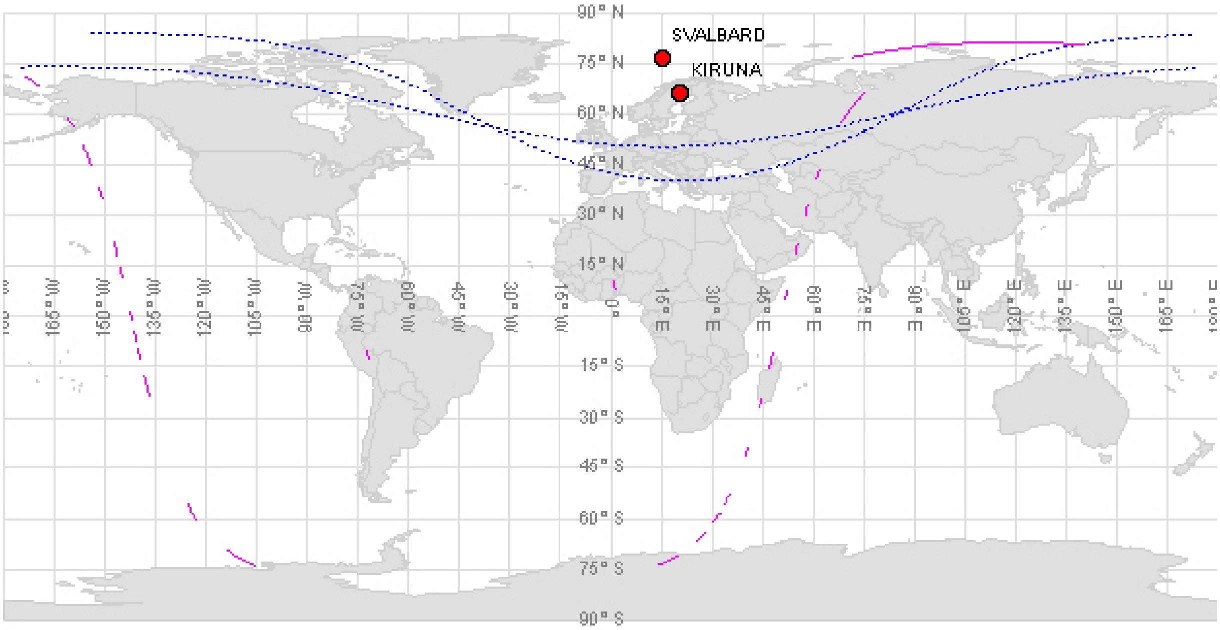

Figure 3.3-2: Orbit segments corresponding to planned data acquisitions for which no GOMOS level 0 product has become available

3.3.2 HIGHER-LEVEL PRODUCTS

Routine dissemination of higher-level products produced by the PDS to Cal/Val teams and other users is enabled. Currently ESA provides the Cal/Val teams with selected products that are generated with the prototype processor developed and operated by ACRI.

4 INSTRUMENT CONFIGURATION AND PERFORMANCE

4.1 Instrument Operation and Configuration

Since end of March 2003 the instrument has suffered some changes in the minimum azimuth range configuration in order to avoid the anomaly "Voice_coil_command_saturation" that caused the instrument to go into STAND BY/REFUSE mode. Since the change to the redundant chain B on July, the full range in azimuth has been again used (table 4.1-1).

Table 4.1-1: Historical changes in Azimuth configuration

Date	Orbit	Minimum Azimuth
29-MAR-2003 17:40	5635	0.0
31-MAY-2003 06:22	6530	+4.0
16-JUN-2003 16:17	6765	+12.0
15-JUL-2003 01:39	7200	-10.8

The operations of the instrument in other modes than occultation mode are identified in table 4.1-2.

There was no new Configurable Table Interface (CTI) uploaded to the instrument. The files used since the beginning of the mission are in table 4.1-3.

Table 4.1-2: GOMOS operations during November 2003

UTC time	Start orbit	Stop orbit	Mode (Asynchronous or Synchronous)	Calibration (CAL) or Dark Sky Area (DSA)
01 Nov 2003 05:36:30	8734	8734	A	DSA81
08 Nov 2003 05:16:22	8834	8841	A	CAL55
15 Nov 2003 04:56:15	8934	8934	A	DSA82
22 Nov 2003 04:36:08	9034	9034	A	DSA83
29 Nov 2003 04:16:01	9134	9134	A	DSA84

Table 4.1-3: Historic CTI files

CTI filename	Dissemination to FOCC
CTI_SMP_GMVIEC20030716_123904_00000000_00000004_20030715_000000_20781231_235959.N1	16-JUL-2003
CTI_SMP_GMVIEC20021104_075734_00000000_00000003_20021002_000000_20781231_235959.N1	06-NOV-2003
CTI_SMP_GMVIEC20021002_082339_00000000_00000002_20021002_000000_20781231_235959.N1	07-OCT-2003
CTI_SMP_GMVIEC20020207_154455_00000000_00000000_20020301_032709_20781231_235959.N1	21-FEB-2002

4.2 Thermal Performance

Since the beginning of the mission the hot pixel and RTS phenomena (see section 4.4.1) are producing a continuous increase of the dark charge signal within the CCD detectors. In order to minimize this effect, three successive CCD cool down were performed in orbits 800 (25th April 2002), 1050 (13th May 2002) and 2780 (11th September 2002) with a total decrease in temperature of 14 degrees.

Fig. 4.2-1 and 4.2-2 display, respectively, the overall temperature variation and the temperature variation around the Ascending Node Crossing (ANX) time with a resolution of 0.4 degrees (coding accuracy for level 0 data). The CCD temperatures during November are slightly higher than the ones registered in October and about one degree higher than November 2002. The expected seasonal variation of the temperatures with amplitude of around one degree can be clearly observed. The peaks that occur mainly in spectrometer B1 and B2 are also to be noted. They happen a little before the ANX for some consecutive orbits and every 8-10 days. Their origin is still not known, as we did not find any correlation between these peaks and other activities carried out by other ENVISAT instruments. The CCD temperature at almost the same latitude location (fig. 4.2-2) is monitored in order to detect any inter-orbital temperature variation.

The decrease observed on 24th March and twice in September in all detectors is after GOMOS switch off periods, when the instrument did not have enough time to reach the nominal temperature before starting the measurements.

The orbital temperature variation of the detector SPB2 (fig. 4.2-3 & 4.2-4) is nominal being the maximum difference between ascending and descending passes around 2.3 degrees. The stability of the temperature during the orbit is important because it affects the position of the interference patterns.

The phenomenon of the interference is present mainly in SPB and this Pixel Response Non-Uniformity (PRNU) is corrected during the processing.

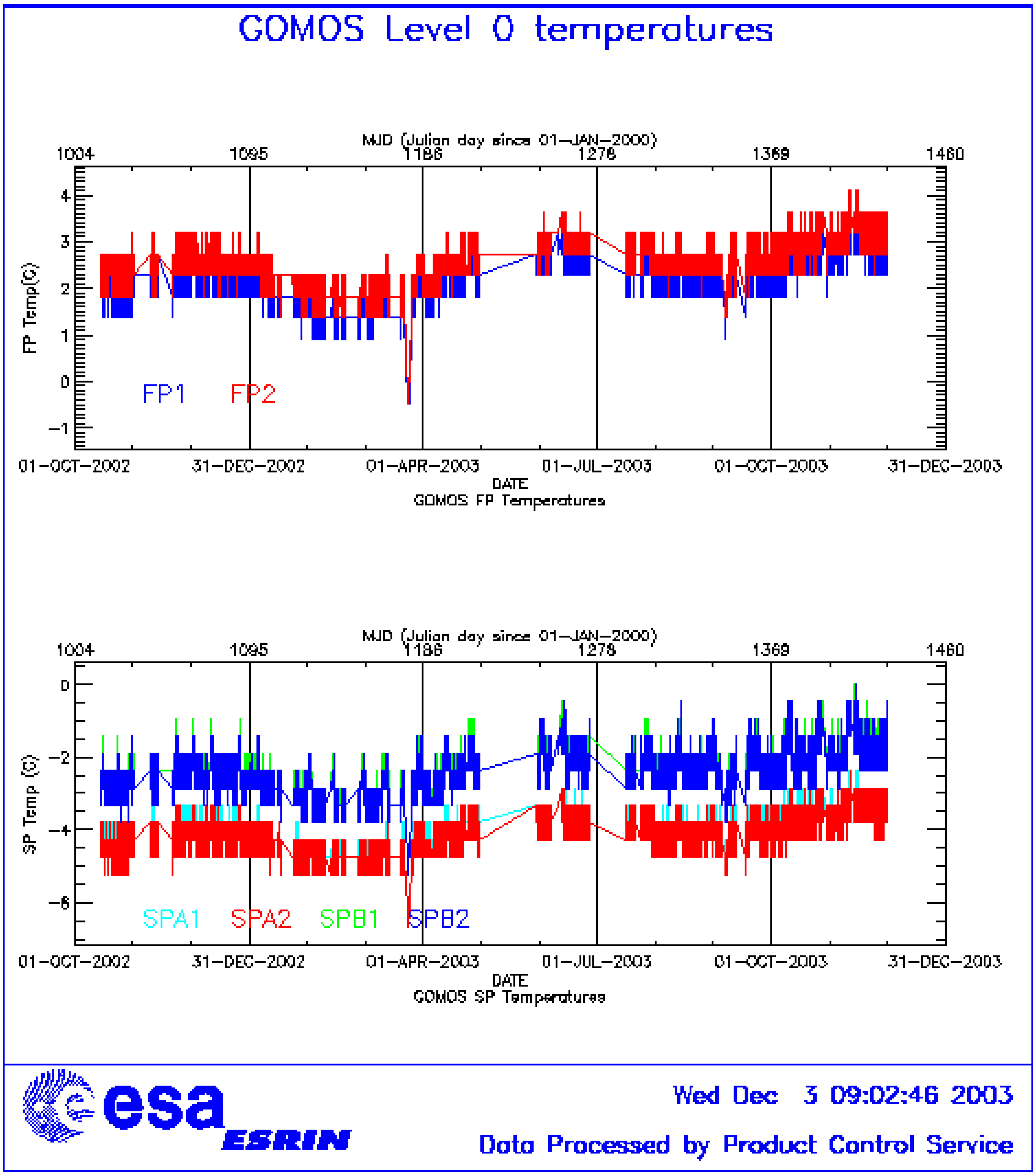

Figure 4.2-1: Level 0 temperature evolution of all GOMOS CCD detectors from October 2002 until end of November 2003

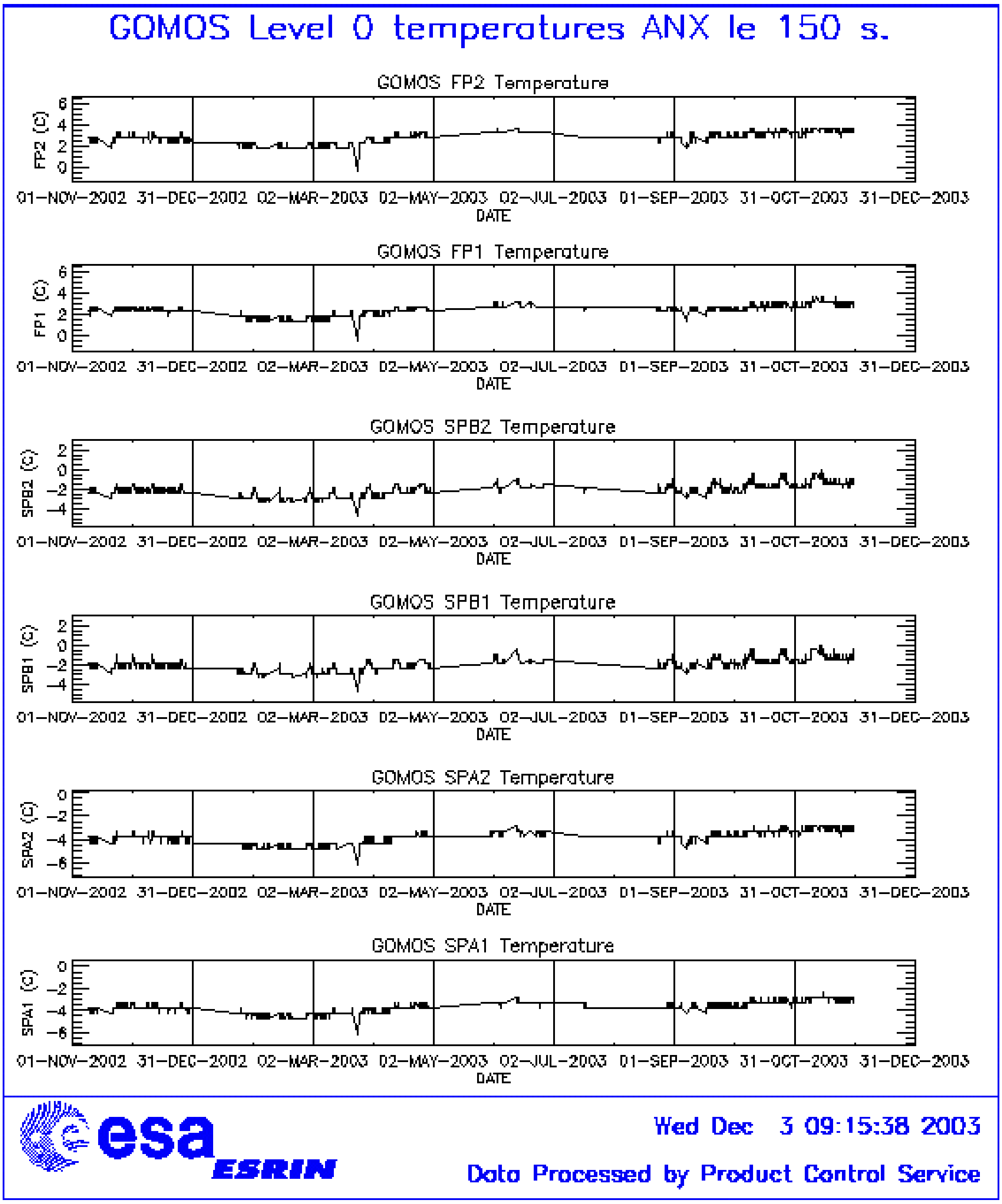

Figure 4.2-2: Level 0 temperature evolution of all GOMOS CCD detectors around ANX from November 2002 until end of November 2003

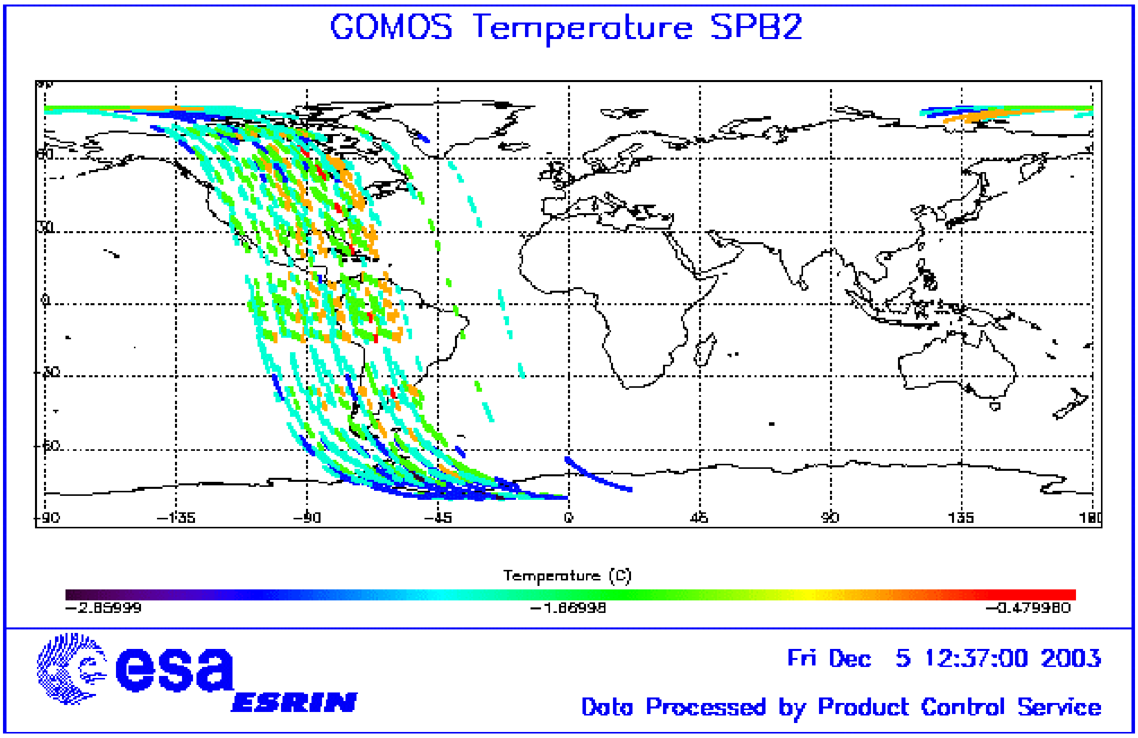

Figure 4.2-3: Ascending orbital variation of SPB2 temperature during some orbits on November 2003

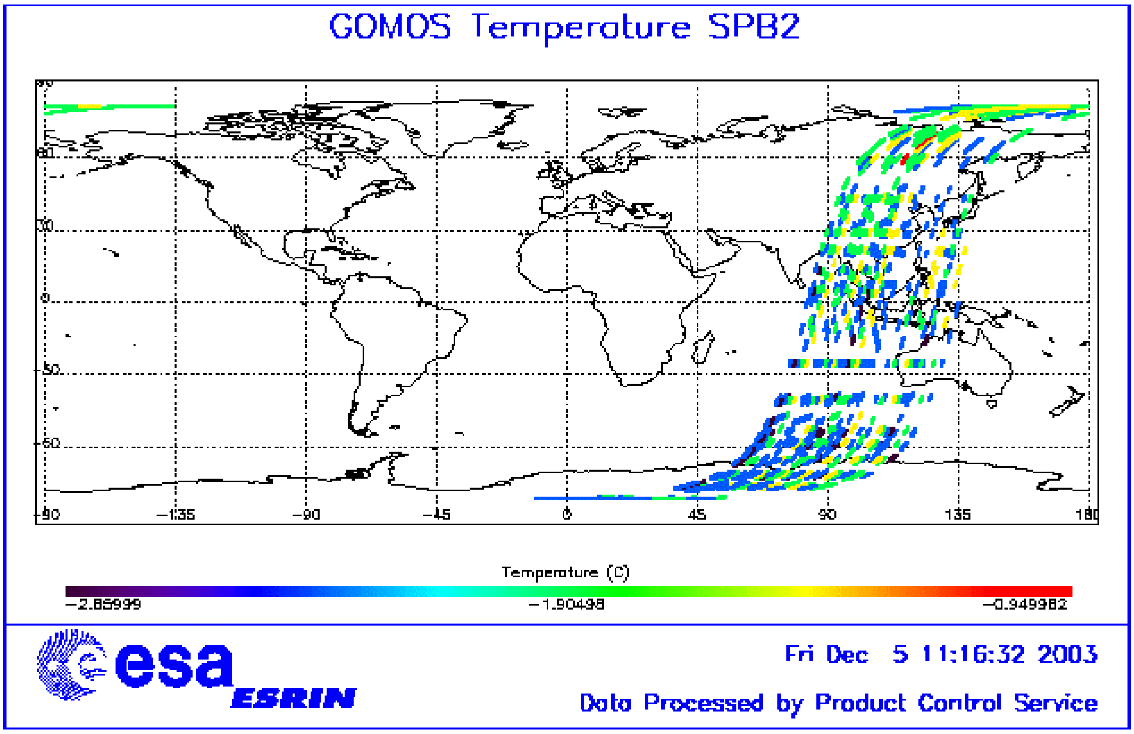

Figure 4.2-4: Descending orbital variation of SPB2 temperature during some orbits on November 2003

4.3 Optomechanical Performance

A new band setting calibration has been performed during November with results that confirm the values of the last calibration analysis done in August.

The position of stellar spectra of star id 2, 9 and 29 observed in dark-limb spatial spread monitoring mode have been averaged above 120 km altitude, and compared to the average positions obtained during the last calibration (blue dots in fig. 4-3.1) performed at the beginning of August after the transition to redundant chain. In table 4.3-1 the mean values of the location of the star signal for all the calibration analysis done till now are reported. The 'left' and 'right' values are calculated (the whole interval is not used) because the spectra present a slight slope, more pronounced in the spectrometer B (see fig. 4-3.1). The current processors GOMOS IPF 4.00 and GOPR prototype 5.4 still expect the spectra to be aligned along CCD lines, and therefore use only a single average line index per CCD. The values currently implemented of 81, 80, 82, 82 for SPA1, SPA2, SPB1 and SPB2 are still compatible with the observed 'left' and 'right' average position. The lookup table implemented in the version 6.0 of the prototype level 1 processor has been updated in order to have the line index as a function of the wavelength.
In table 4.3-2, mean values of the location of the star signal are calculated for some specific wavelength intervals. These intervals have been changed between the calibration performed in September 2002 and the ones performed afterwards. The results obtained are very similar to the ones obtained in previous exercises.
Table 4.3-3 reports the average location of the star spot on the photometer 1 and 2 CCD. No difference has been found for both photometers in column and in row positions.

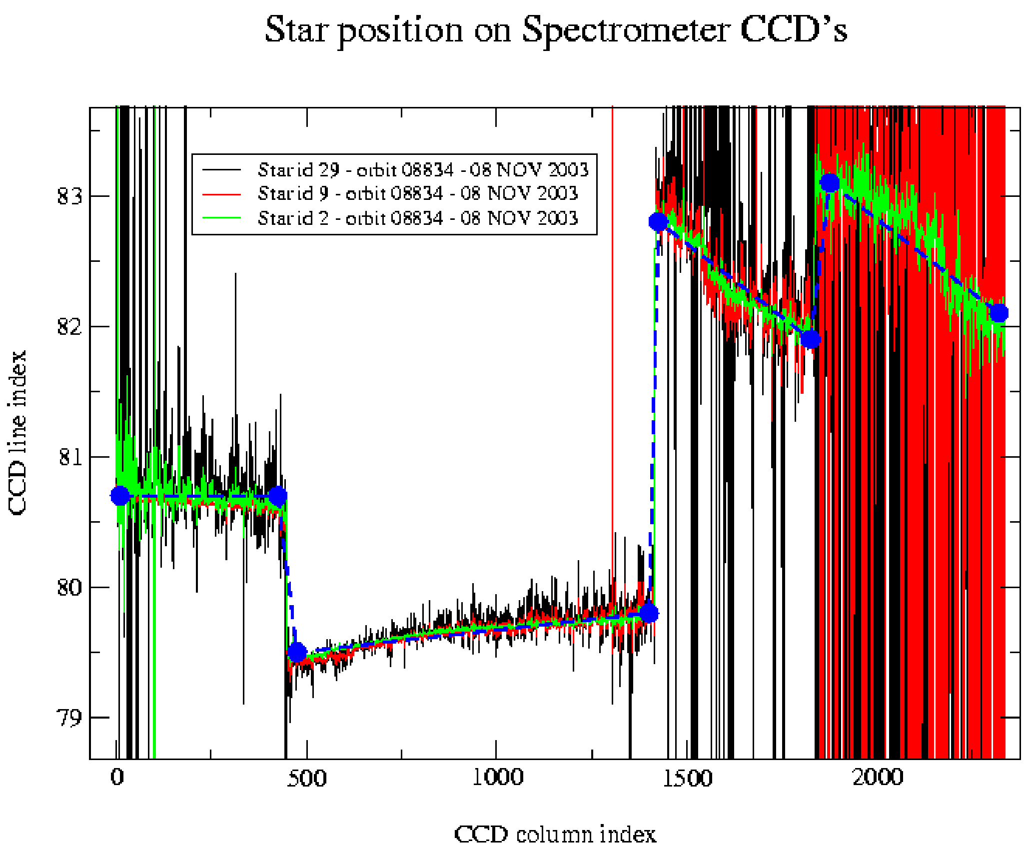

Figure 4.3-1: Average position of star spectra on the CCD

Table 4.3-1: Mean value of the location of the star signal during the occultation at the edges of every band (mean over 50 values, filtering the outliers)

	UV (SPA1) left/right	VIS (SPA2) left/right (Inverted spectra)	IR1 (SPB1) left/right	IR2 (SPB2) left/right
11/09/2002	80.7/80.7	79.8/79.5	82.8/81.9	83.1/82.1
01/01/2003	80.7/80.6	79.8/79.5	82.8/82.0	83.2/82.2
17/07/2003 & 02/08/2003	80.7/80.7	79.8/79.5	82.8/81.9	83.1/82.1
08/12/2003	80.7/80.6	79.8/79.5	82.8/81.9	83.1/82.1

Table 4.3-2: Mean value of the location of the star signal during the occultation (as table 4.3-1) but now within some wavelength intervals

	UV (SPA1)	VIS (SPA2)	IR1 (SPB1)	IR2 (SPB2)
11/09/2002 **wl range (nm)**	80.8 [300-330]	79.8 [500-530]	82.6 [760-765]	82.9 [937-942]
01/01/2003 **wl range (nm)**	80.6 [350-360]	78.6 [650-670]	81.6 [760-765]	80.3 [935-945]
02/08/2003	80.6	79.7	82.5	82.8
08/11/2003	80.6	79.9	82.4	82.8

Table 4.3-3: Average column and row pixel location of the star spot on the photometer CCD during the occultation

	FP1 (column/row)	FP2 (column/row)
11/09/2002	11/4	5/5
01/01/2003	10/4	6/4.9
02/08/2003	10/4	6/5
08/11/2003	10/4	6/5

4.4 Electronic Performance

4.4.1 DARK CHARGE EVOLUTION AND TREND

The trend of Dark Charge (DC) is of crucial importance for the final quality of the products, and is therefore subject to intense monitoring. As part of the DC there is:

- “Hot pixels”, a pixel is “hot” when its dark charge exceeds its value measured on ground, at the same temperature, by a significant amount.
- RTS phenomenon (Random Telegraphic Signal), it is an abrupt change (positive or negative) of the CCD pixel signal, random in time, affecting only the DC part of the signal and not the photon generated signal.

The temperature dependence of the DC would make this parameter a good indicator of the DC behaviour, but the hot pixels and the RTS are producing a continuous increase of the DC (see trend in fig. 4.4-1 and 4.4-2). To take into account these phenomena, in the last version of the level 1 processor (GOMOS/4.00) operational since May 2003, a DC map per orbit is extracted from a Dark Sky Area (DSA) observation performed around ANX (full dark conditions). For every level 1b product (occultation), the actual thermistor temperature of the CCD is used to convert the DC map measured around ANX into an estimate of the DC at the time (and different temperature) of the actual occultation. When the DSA observation is not available, the DC map inside the calibration product that was measured at a given thermistor reference temperature is used; again, the actual thermistor temperature of the CCD is used to compute the actual map.

In fig. 4.4-1 and 4.4-2 it is plotted the average DC inserted by the processor into the level 1b data products for the spectrometers SPA1 and SPB2 (per band: upper, central and lower). From the figures, it can be noted that the rate of increase of DC for the last two months, October/November, is higher that the rate of August/September.

The same DC values are plotted in fig. 4.4-3 but for some occultations only during the reporting period.

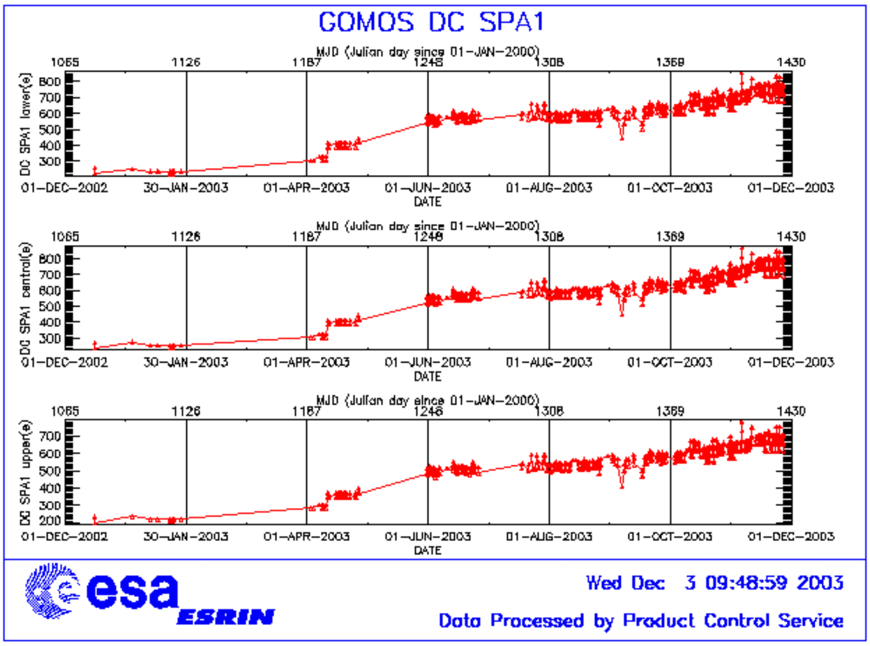

Figure 4.4-1: Mean DC evolution on SPA1 from 15th December 2002 until end of November 2003

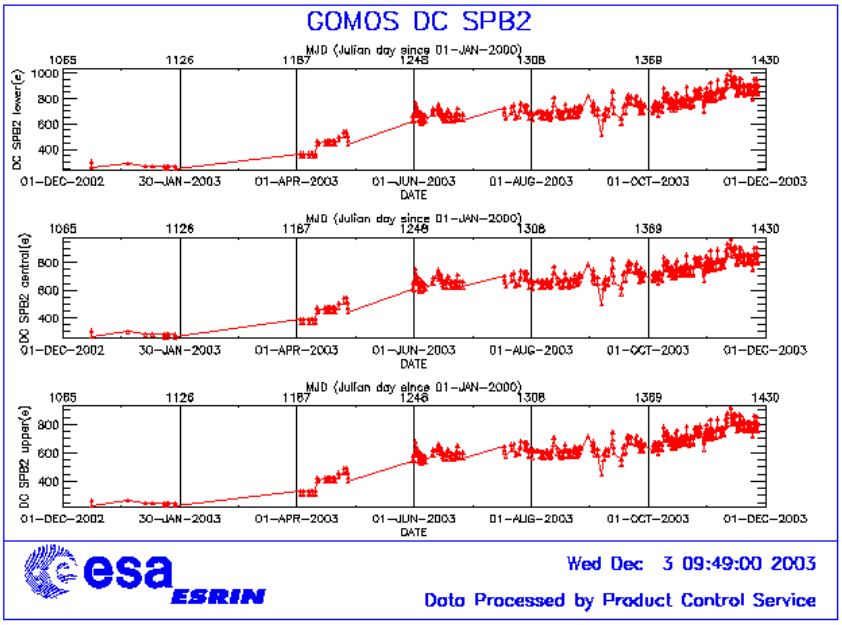

Figure 4.4-2: Mean DC evolution on SPB2 from 15th December 2002 until end of November 2003

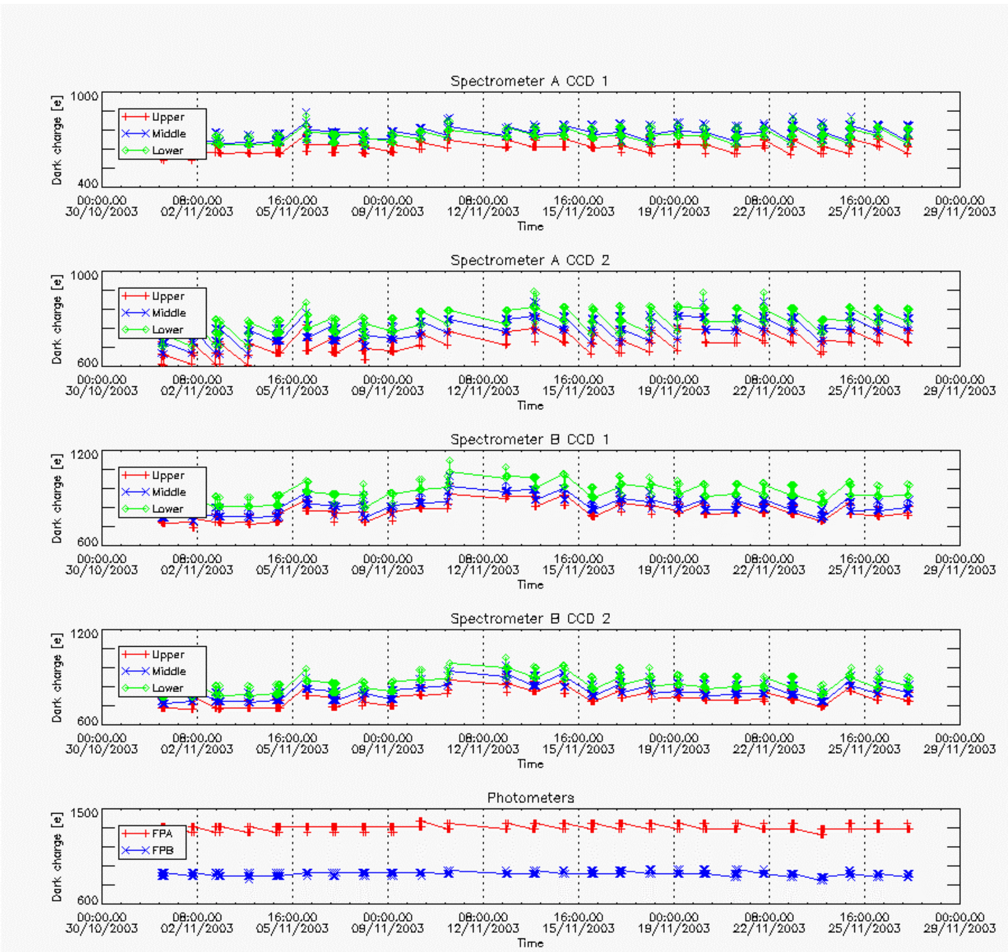

Figure 4.4-3: Mean Dark Charge of spectrometers and photometers during November 2003

4.4.2 SIGNAL MODULATION

A parasitic signal was found to be systematically present, added to the useful signal, at least for spectrometers A1 and A2. The modulation is corrected in the data processing, but the modulation signal standard deviation is routinely monitored in order to detect any trend (fig. 4.4-4).

The modulation standard deviation, for every spectrometer, is characterised as follows:

$$\sigma_{mod} = (\text{'static noises'} - \text{'total static variance'})^{1/2} / \text{gain} \qquad \text{(in ADU)}$$

- The 'static noises' are calculated from the DSA observation performed once per orbit
- The 'total static variance' is obtained from ADF data (electronic chain noise, quantization noise).

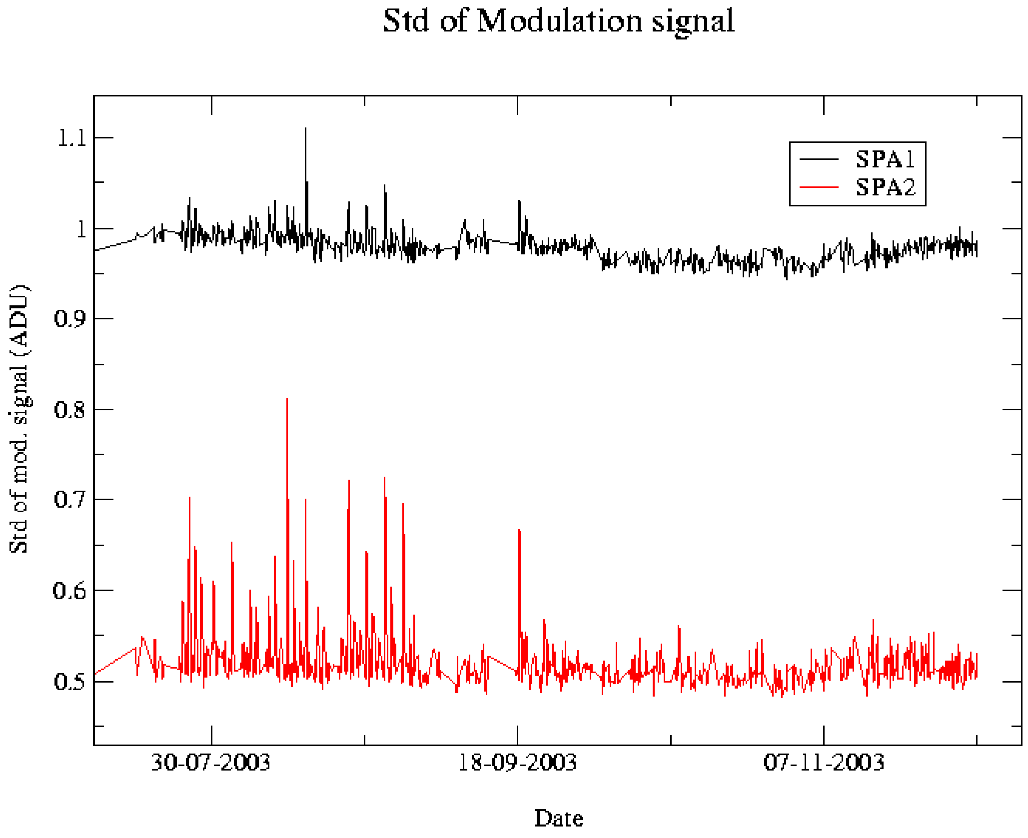

Figure 4.4-4: Standard deviation of the modulation signal

4.4.3 ELECTRONIC CHAIN GAIN AND OFFSET

No new electronic chain gain and offset calibration has been done during the reporting month so these results have been already presented in previous MR.

The routine monitoring of the ADC offset is a good indicator of the ageing of the instrument electronics. During the definition of this routine activity, an exercise has been done to analyze the

variation of the ADC offset using the calibration observation in linearity mode (orbits 2810, 4384, 4834, 5219 and 5734).
The fig. 4.4-5 presents the evolution of the calibrated ADC offset for each spectrometer electronic chain. The unexpected increase of this offset seems to be due to an external contribution. In the ADC offset calibration procedure, linearity observations are used with two integration times of 0.25 and 0.50 seconds to extrapolate to an integration time of 0 seconds that give the complete chain offset and not only the ADC offset. The complete offset contains any possible offsets, and especially the static dark charge (i.e. the dark charge that does not depend of the spectrometer integration time). If the memory area of the CCD is affected by the generation of hot pixels (this is confirmed by the presence of vertical lines visible in the measurement maps in spatial spread monitoring mode), it becomes that the increase observed in fig. 4.4-5 is due to these new hot pixels.

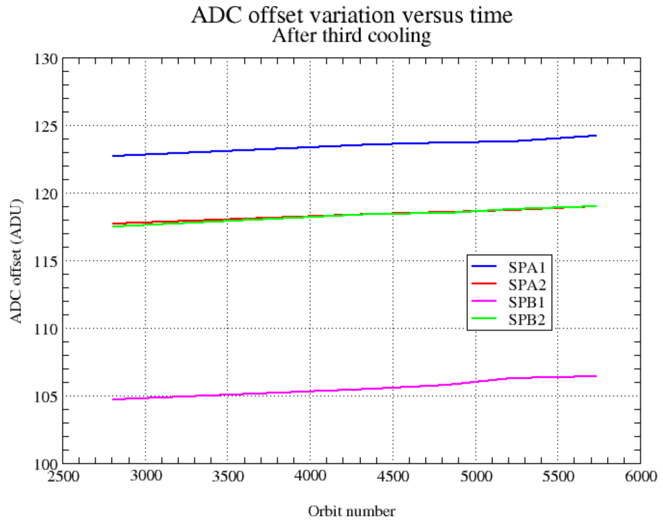

Figure 4.4-5: Evolution of the ADC offset for each spectrometer electronic chain

Next task consists in completing the analysis to confirm that the offset increase is due to the hot pixels in memory area. This can be proven by the study of the noise due to the increased dark charge. The increase of ADC offset will be assumed to be equal to the increase of 'static dark charge' and the corresponding noise will be computed and compared to the increase of the signal variance residual.

If we keep the ADC offset constant, as it is also used to compute the dark charge at band level used to correct the samples in the level 1b processing, the increase of the static dark charge - not taken into account in the ADC offset - is compensated by an artificial increase of the calibrated dark charge. So, the star and limb spectra are correctly corrected for dark charge. A small bias can be added to the instrument noise due to the incorrect dark charge level. Anyway, this quantity is not large enough to require a modification of the ADC offset value.

4.5 *Acquisition, Detection and Pointing Performance*

4.5.1 SATU NOISE AND EQUIVALENT ANGLE

The Star Acquisition and Tracking Unit (SATU) noise equivalent angle (SATU NEA) consists of the statistical angular variation of the SATU data above the atmosphere.
The mean of the standard deviation (std over the 50 values per measurement) above 105 km are computed for every occultation, giving two values per occultation: one in the 'X' direction, one in the 'Y' direction. A mean value per day in every direction is calculated and monitored in order to assess instrument performance in terms of star pointing. The thresholds are 2 and 3 micro radians in 'X' and 'Y' directions respectively. Before May 2003, data above 90 km have been considered (instead of 105 km) but from May 2003 on, data taken in the mesospheric oxygen layer (located around 100 km altitude) have been avoided because they could cause fluctuations on the SATU data. Also the products with errors (error flag set) are discarded from May 2003 onwards.
It can be seen in fig. 4-5.1 that the SATU NEA had some increase during the month but still well below the thresholds.
The results for some occultations belonging to previous months (monthly averages) are presented in fig. 4.5-2, where no trend is visible so far.

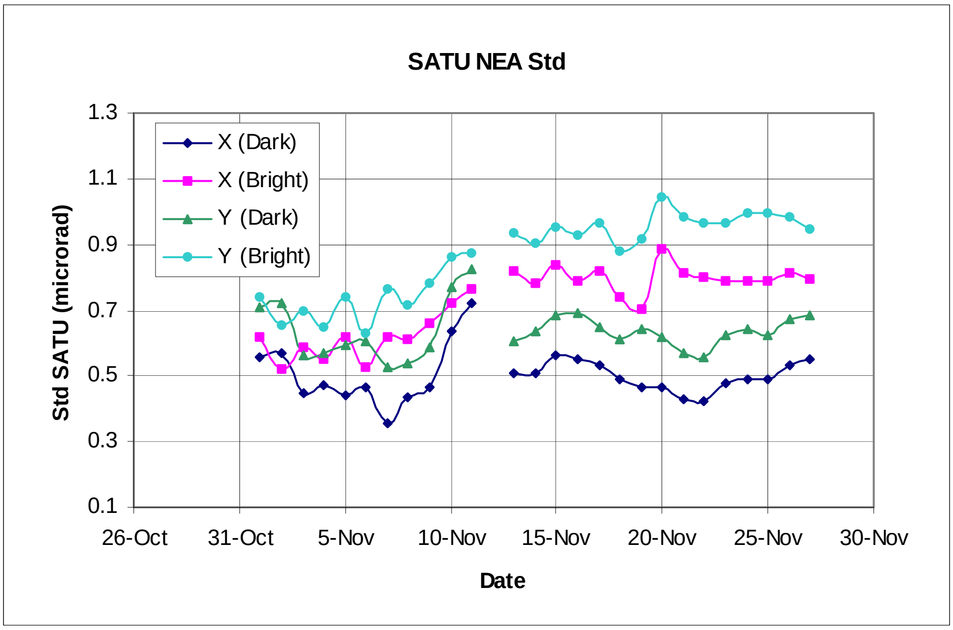

Figure 4.5-1: Average value per day of SATU NEA std above 105 kms

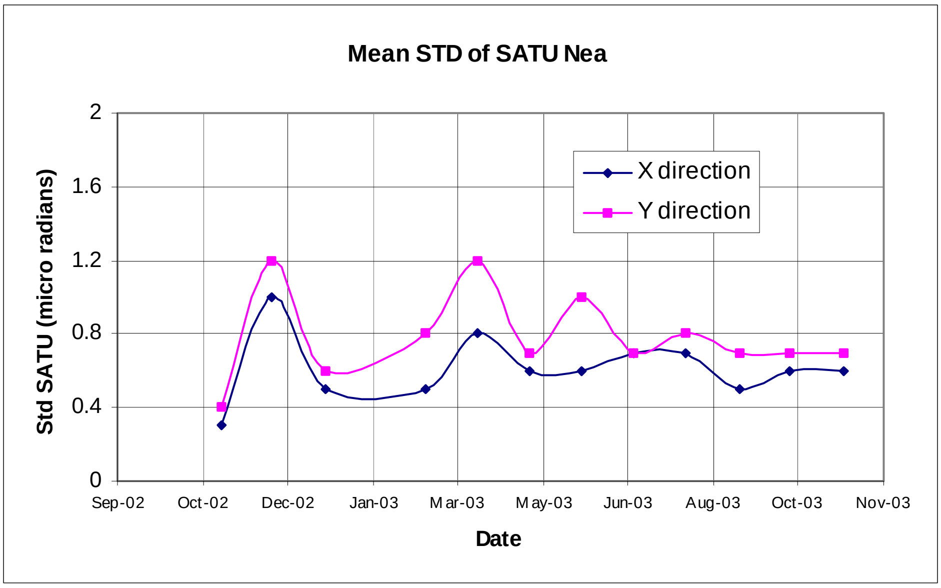

Figure 4.5-2: Average value per month of SATU NEA std above 105 km

4.5.2 TRACKING LOSS INFORMATION

This verification consists of the monitoring of the tangent altitude at which the star is lost. It is an indicator of the pointing performance although it is to be considered that star tracking is also lost due to the presence of clouds and hence not only due to deficiencies in the pointing performance. Therefore, only the detection of any systematic long-term trend is the main purpose of this monitoring. The recent results are presented in fig. 4.5-3 and fig. 4.5-4:

- The dependence of the altitude at which tracking is lost on the magnitude of the star is very small because the tracking is mainly lost due to the refraction and the scintillation that depend on the atmospheric conditions.
- The majority of the stars lost at high altitude (above 30 km) in fig. 4.5-3 belong to very long lasting occultations (very oblique ones) so it is not a fact related to deficiencies in pointing. There is only one point in the same plot that belongs to a short occultation (star id 52 on 01st November).
- In fig. 4.5-4 there are no stars lost at high tangent altitude.
- Some statistics are given in fig. 4.5-5 calculated for a set of data and not for the whole months. For the moment, no trend is visible in the plot.

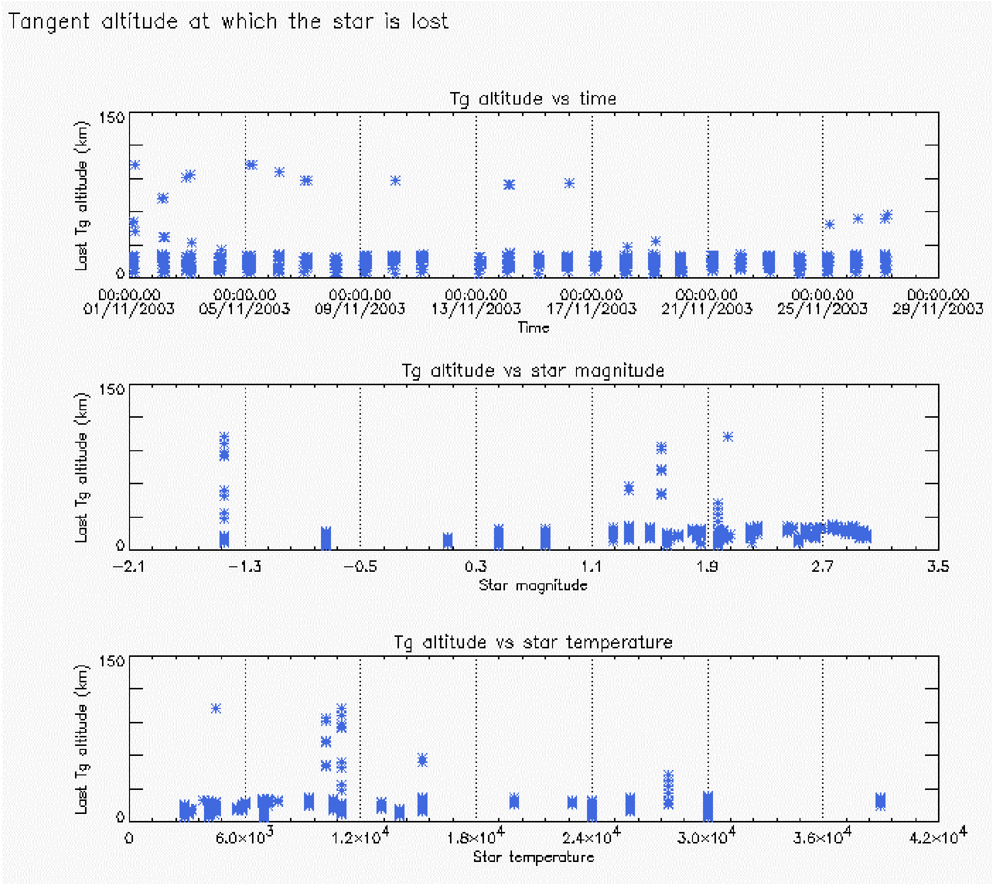

Figure 4.5-3: Last tangent altitude of the occultation (dark limb), point at which the star is lost

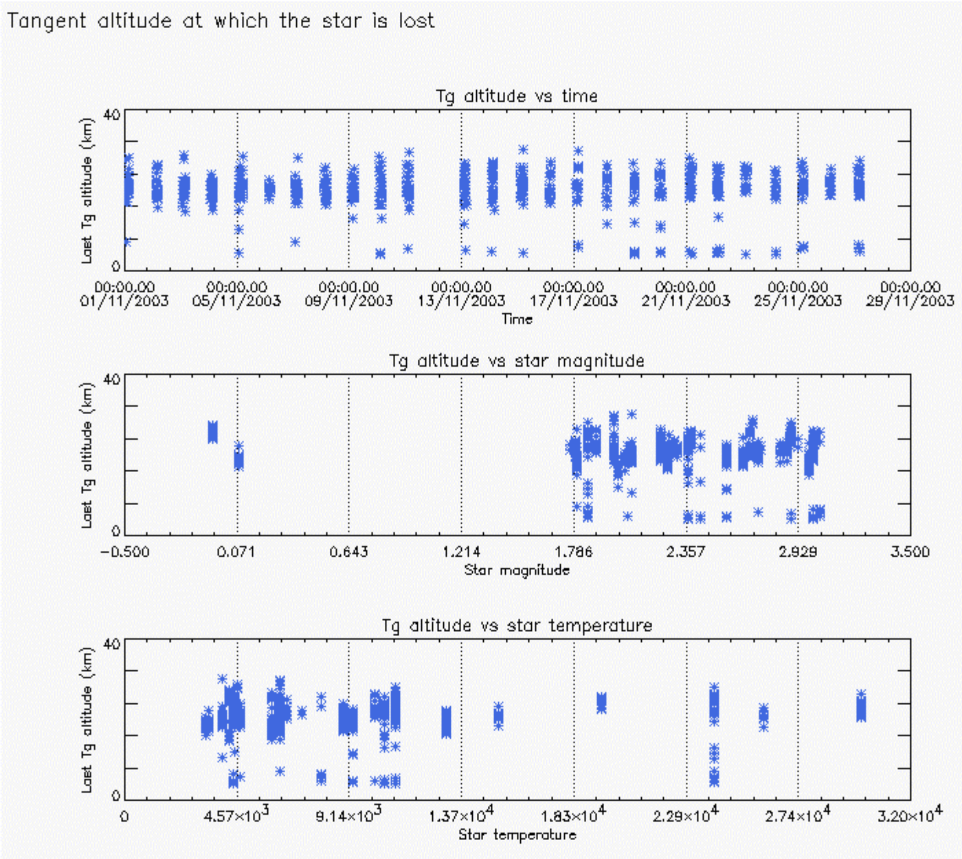

Figure 4.5-4: Last tangent altitude of the occultation (bright limb), point at which the star is lost

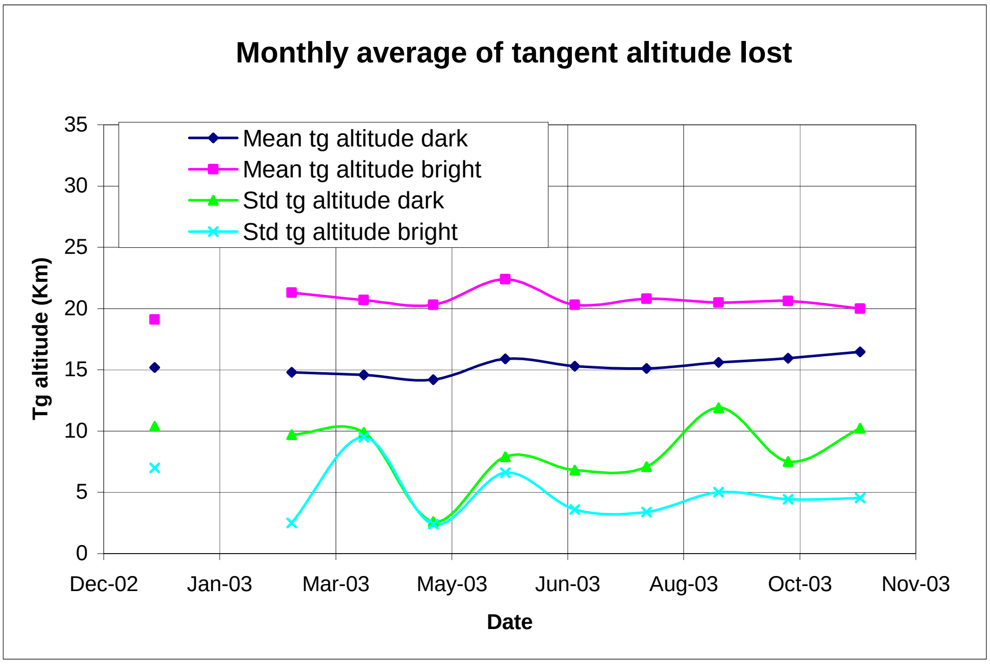

Figure 4.5-5: Monthly mean tangent altitude (and Std) at which the star is lost for some occultations since January 2003

4.5.3 MIP (MOST ILLUMINATED PIXEL)

The MIP (Most Illuminated Pixel) is the star position on the SATU CCD in detection mode and it is recorded in the housekeeping data. The nominal centre of the SATU is pixel number **145** in elevation and number **205** in azimuth. The detection of the stars should not be far from this centre. As can be seen in fig. 4.5-6 the azimuth is always well within the threshold (table 4.5-1) since September 2002 even if a small variation is present. The elevation MIP has a significant variation and now the stars are detected 5 pixels above the SATU centre. The variation in MIP positions seems to be seasonal and it is an indicator of deviations from expected ENVISAT platform attitude. A de-pointing of 0.1 degrees corresponds to a MIP variation onto the SATU CCD of 50 pixels. The MIP displacement will be carefully monitored. Fig. 4.5-7 shows the standard deviation of azimuth and elevation that should be within the thresholds of table 4.5-1. The peaks observed mean that one (or more) stars where detected very far from the SATU centre and, in this case, the star/s is lost during the centering phase (see section 3.2 for stars lost in centering).

Table 4.5-1: MIP thresholds

MIP X: mean delta Az	[198 - 210]
Std delta Az	7
MIP Y: mean delta El	[145 – 154]
Std delta El	4

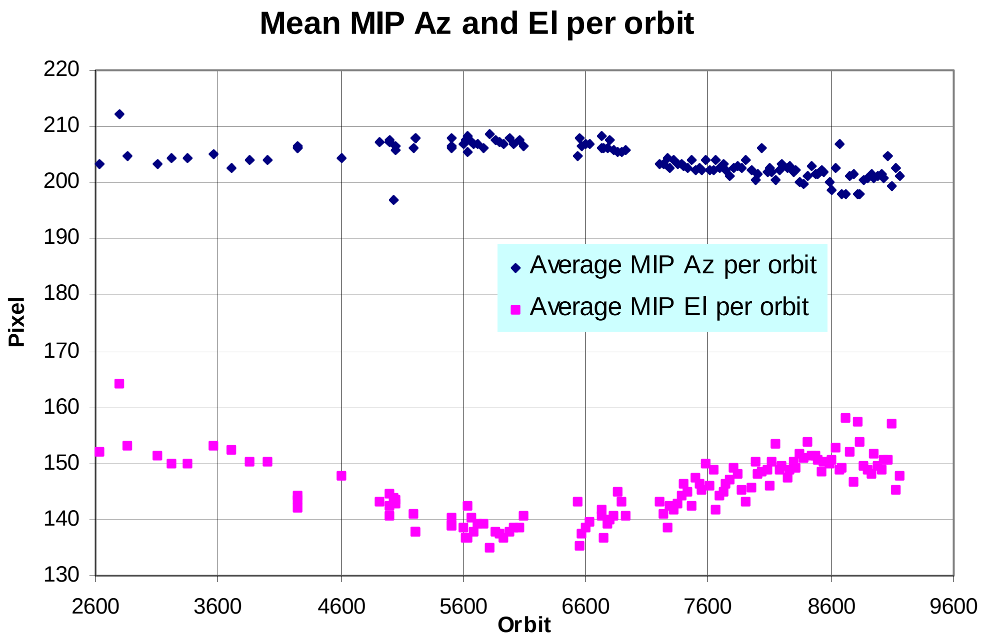

Figure 4.5-6: Mean values of MIP for some orbits since 1st September 2002 (see table 4.5-1)

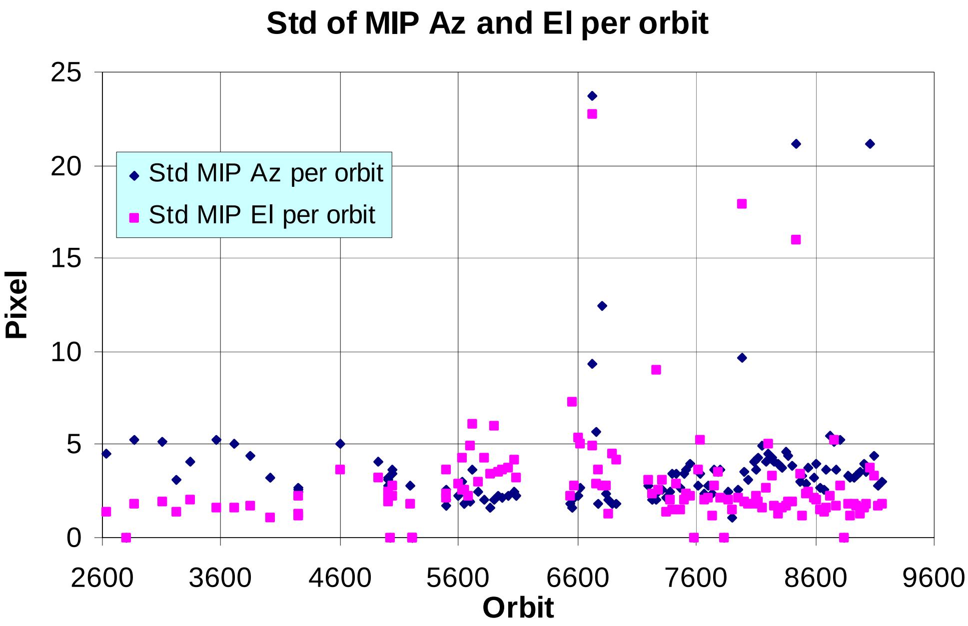

Figure 4.5-7: Standard deviation of MIP Azimuth and Elevation for some orbits since 1st September 2002 (see table 4.5-1)

5 LEVEL 1 PRODUCT QUALITY MONITORING

5.1 Processor Configuration

5.1.1 VERSION

About 10% of GOM_TRA_1P products have been received in the PCF for routine quality control and long term trend quality monitoring. The current level 1 processor software version for the operational ground segment is GOMOS/4.00 (see table 5.1-1) and the product specification is PO-RS-MDA-GS2009_10_3H. This processor has been cleared for initial level 1 data release, with a disclaimer for known artefacts that are currently being resolved and will be implemented in the next release (http://envisat.esa.int/dataproducts/availability).

Cal/Val teams are supplied with selected data sets generated by the prototype processor GOPR 5.4. See table 5.1-2 for the prototype level 1b versions and modifications.

Table 5.1-1: PDS level 1b product version and main modifications implemented

Date	Version	Description of changes
31-MAY-2003	Level 1b version 4.00 at PDHS-E and PDHS-K	Algorithm baseline level 1b DPM 5.4: • Modulation correction step added after the cosmic rays detection processing • Inversion of the non-linearity and offset corrections • Modification of the computation of the estimated background signal measured by the photometers: use the spectrometer radiometric sensitivity curve and the photometer transfer function. • Use of the dark charge map at orbit level computed from the DSA (dark sky area) if any in the level 0 product • Implementation of a new unfolding algorithm for the photometer samples • See ref. [2] for more details
21-NOV-2002	Level 1b version 3.61 at PDHS-E and PDHS-K	Algorithm baseline DPM 5.3: • Review of some default values • New definition of one PCD flag (atmosphere) • Temporal interpolation of ECMWF data • See ref. [2] for more details

Table 5.1-2: GOPR level 1b product version and main modifications implemented

Date	Version	Description of changes
25-JUL-2003	GOPR 5.4f	• The demodulation process is applied only in full dark limb and twilight limb conditions.
17-JUL-2003	GOPR 5.4e	• Sun zenith angle is computed in the geolocation process. The occultation is now classified into (0) full dark limb condition, (1) bright limb condition and (2) twilight limb condition. • No background correction applied in full dark limb condition. The location of the image of the star spectrum on the CCD array is no more aligned with the CCD lines.
02-JUL2003	GOPR 5.4d	• The maximum number of measurements is set to 509 (instead of 510) in the GOPR prototype.
17-MAR-2003	GOPR 5.4c	• Modification of the CAL ADFs (update of the limb radiometric LUT). The products are affected only if the limb spectra are converted into physical units • Modifications to allow compatibility with ACRI computational cluster (no modifications of the results) • Modification of the logic to handle dark charge map refresh at orbit level (DSA data is now directly processed by the level 1b processor if available in the level 0 product). No impact on the results
21-FEB-2003	GOPR 5.4b	• DC map values are rounded when written in the level 1b product • Modification of the CAL ADFs (update of the wavelength assignment of SPB1 and SPB2) • Modify the computation of flag_mod in the modulation correction routine
17-JAN-2003	GOPR 5.4a	• use the start and stop dates of the occultation when calling the CFI interpol instead of start and stop dates of the level 0 product • modify the ECMWF filename information in the SPH of the level 1b and limb products

5.1.2 AUXILIARY DATA FILES (ADF)

The ADF's files in tables 5.1-3, 5.1-4, 5.1-5, 5.1-6 and 5.1-7 have been disseminated to the PDS during the whole mission. For every type of file, the validity runs from the start validity time until the start validity time of the following one, but if an ADF file has been disseminated after the start validity time, it is obvious that it will be used by the PDS only after the dissemination time (this happens the majority of the times). As the other ADF's, the calibration auxiliary file (GOM_CAL_AX) has been updated several times in the past (table 5.1-7) but the difference is that now it is updated in a weekly basis with only new DC maps, and that is why the files used in November are reported in a separate table (table 5.1-8) that will change from month to month. On 10th, 17th and 24th November new calibration ADF's were disseminated with updated DC map of orbits 08852, 08941 and 09050 respectively (table 5.1-8).

The files outlined in yellow are the set of auxiliary files used during the month of November.

Table 5.1-3: Table of historic GOM_PR1_AX files used by PDS for level 1b products generation

Used by PDS for Level 1b products generation in period	GOM_PR1_AX (GOMOS processing level 1b configuration file)
01-MAR-2002 → 29-MAR-2002	GOM_PR1_AXVIEC20020121_165314_20020101_000000_20200101_000000 • Pre-launch configuration
30-MAR-2002 → 14-NOV-2002	GOM_PR1_AXVIEC20020329_115921_20020324_200000_20100101_000000 • Changed num_grid_upper, thr_conv and max_iter in the atmospheric GADS
Not used	GOM_PR1_AXVIEC20020729_083756_20020301_000000_20100101_000000 • Cosmic Ray mode + threshold • DC correction based on maps • Non-linearity correction disabled
Not used	GOM_PR1_AXVIEC20021112_170331_20020301_000000_20100101_000000 • Central background estimation by linear interpolation + associated thresholds
15-NOV-2002 → 26-MAR-2003	GOM_PR1_AXVIEC20021114_153119_20020324_000000_20100101_000000 • Same content as GOM_PR1_AXVIEC20021112_170331_20020301_000000_20100101_000000 but validity start updated so as to supersede according to the PDS file selection rules GOM_PR1_AXVIEC20020329_115921_20020324_200000_20100101_000000
27-MAR-2003	GOM_PR1_AXVIEC20030326_085805_20020324_200000_20100101_000000 • Same content as GOM_PR1_AXVIEC20021112_170331_20020301_000000_20100101_000000 but validity start updated so as to supersede according to the PDS file selection rules GOM_PR1_AXVIEC20020329_115921_20020324_200000_20100101_000000

Table 5.1-4: Table of historic GOM_INS_AX files used by PDS for level 1b products generation

Used by PDS for Level 1b products generation in period	GOM_INS_AX (GOMOS instrument characteristics file)
01-MAR-2002 → 29-JUL-2002	GOM_INS_AXVIEC20020121_165107_20020101_000000_20200101_000000 • Pre-launch configuration
30-JUL-2002 → 12-NOV-2002	GOM_INS_AXVIEC20020729_083625_20020301_000000_20100101_000000 • Factors for the conversion of the SFA angles from SFM axes to GOMOS axes
13-NOV-2002 → 16-JUL-2003	GOM_INS_AXVIEC20021112_170146_20020301_000000_20100101_000000 • No more invalid spectral range
Not used	GOM_INS_AXVIEC20030716_080112_20030711_120000_20100101_000000 • New value for SFM elevation zero offset for redundant chain: 10004
17-JUL-2003	GOM_INS_AXVIEC20030716_105425_20030716_120000_20100101_000000 • Bias induct azimuth redundant value set to -0.0084 rad (-0.4813 deg)

Table 5.1-5: Table of historic GOM_CAT_AX files used by PDS for level 1b products generation

Used by PDS for Level 1b products generation in period	GOM_CAT_AX (GOMOS Stat Catalogue file)
01-MAR-2002	GOM_CAT_AXVIEC20020121_161009_20020101_000000_20200101_000000 • Pre-launch configuration

Table 5.1-6: Table of historic GOM_STS_AX files used by PDS for level 1b products generation

Used by PDS for Level 1b products generation in period	GOM_STS_AX (GOMOS Star Spectra file)
01-MAR-2002	GOM_STS_AXVIEC20020121_165822_20020101_000000_20200101_000000 • Pre-launch configuration

Table 5.1-7: Table of historic GOM_CAL_AX files used by PDS for level 1b products generation

Used by PDS for Level 1b products generation in period	GOM_CAL_AX (GOMOS Calibration file)
01-MAR-2002 → 29-JUL-2002	GOM_CAL_AXVIEC20020121_164808_20020101_000000_20200101_000000 • Pre-launch configuration
Not used	GOM_CAL_AXVIEC20020121_142519_20020101_000000_20200101_000000 • Pre-launch configuration
30-JUL-2002 → 12-NOV-2002	GOM_CAL_AXVIEC20020729_082426_20020717_193500_20100101_000000 • Band setting information • Wavelength assignment • Spectral dispersion LUT • ADC offset for Spectrometers • PRNU maps • Thermistor coding LUT • DC maps

Not used	GOM_CAL_AXVIEC20021112_165603_20020914_000000_20100101_000000 • Band setting information • DC maps • PRNU maps • Wavelength assignment • Spectral dispersion LUT • Radiometric sensitivity LUT (star and limb) • SP-FP intercalibration LUT • Vignetting LUT • Reflectivity LUT • ADC offset
13-NOV-2002 → 30-JAN-2003	GOM_CAL_AXVIEC20021112_165948_20021019_000000_20100101_000000 • Only DC maps updated
31-JAN-2003 → 11-APR-2003	GOM_CAL_AXVIEC20030130_133032_20030101_000000_20100101_000000 • Only DC maps updated (using DSA of orbit 04541)
12-APR-2003 → 02-JUN-2003	GOM_CAL_AXVIEC20030411_065739_20030407_000000_20100101_000000 • Modification of the radiometric sensitivity curve for the limb spectra. Note that the modification of this LUT has no impact on the GOMOS processing. The LUT is just copied into the level 1b limb product for user conversion purpose. • Updated DC map only (using DSA of orbit 05762).
03-JUN-2003: from this date onwards, only updates to DC maps are done. Every month, the table of new GOM_CAL files with only DC maps updated is provided (table 5.1-8)	GOM_CAL_AXVIEC20030602_094748_20030531_000000_20100101_000000 • Updated DC maps only (using DSA of orbit 06530)

Table 5.1-8: Calibration ADF for November 2003. These files are updated (only with DC maps) in a 8-10 days basis

Used by PDS for Level 1b products generation in period	GOM_CAL_AX (GOMOS Calibration file)
30-OCT-2003 → 10-NOV-2003	GOM_CAL_AXVIEC20031030_133050_20031027_000000_20100101_000000 (Orbit 08695, 29-OCT-2003)
11-NOV-2003 → 17-NOV-2003	GOM_CAL_AXVIEC20031110_084900_20031107_000000_20100101_000000 (orbit 08852, 07-NOV-2003)
18-NOV-2003 → 24-NOV-2003	GOM_CAL_AXVIEC20031117_155226_20031114_000000_20100101_000000 (orbit 08941, 14-NOV-2003)
25-NOV-2003	GOM_CAL_AXVIEC20031124_155405_20031121_000000_20100101_000000 (orbit 09050, 23-NOV-2003)

5.2 Quality Flags monitoring

In this section it is monitored some Product Quality information stored in the level 1b products that are not flagged (MPH error flag not set). The products flagged are around 1.7% of the products received for the quality monitoring.

On the one hand, for every product we have information of the **number of measurements** where a given problem was detected (i.e. number of invalid measurements, number of measurements containing saturated samples, number of measurements with demodulation flag set…). On the other hand, there are **flags** that indicate problems within the product (i.e. flag set to one if the reference spectrum was computed from DB, flag set to zero if SATU data were not used…).

For the information on the number of measurements a plot (percentages) is provided in fig. 5.2-1. It can be seen that the cosmic rays hits occurred often for the 95% of the measurements of the product. Another observation that can be done is that, for many products, the 30 % of the measurements have the star signal falling outside the central band. The other values (% of invalid measurements per product, % of measurements per product with datation errors…) are quite low.

The flag information is given in table 5.2-1. It is reported also the percentage of the products that have at least one measurement with demodulation flag set.

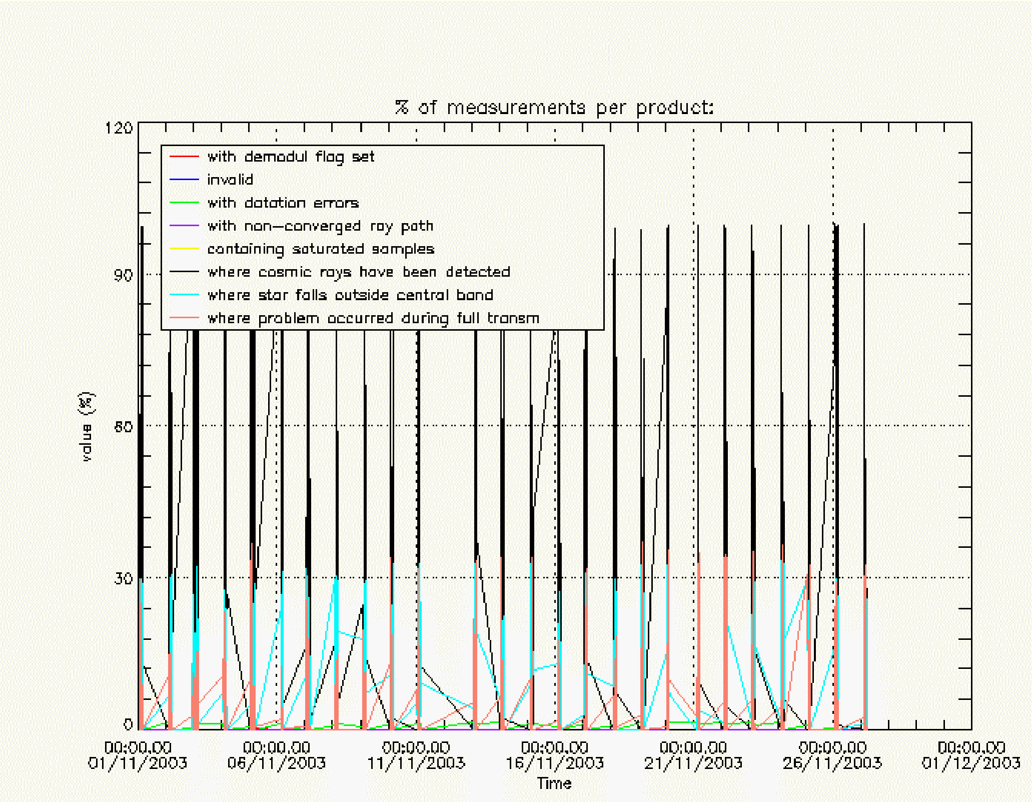

Figure 5.2-1: Level 1b product quality monitoring

Table 5.2-1: Percentage of products during the reporting period with:

At least one measurement with demodulation flag set:	17.1863 %
Reference spectrum computed from DB:	0.00000 %
Reference spectrum with small number of measurements:	0.00000 %
SATU data not used:	0.00000 %

5.3 Spectral Performance

No new spectral calibration has been done during November. These results were already presented in previous versions of the MR with nominal results thus far.

The values reported (table 5.3-1) are, for every star ID (1, 2, 4, 9, 18, 25), the wavelength of the first useful pixel of SPA2. This value is calculated by addition to the actual wavelength assignment, the spectral shift for which a maximum correlation has been found between the reference spectrum and the one of the occultation. It can be observed in table 5.3-1 that for all the stars (but for star id 4) the difference between the actual wavelength (690.492981 nm) and the one reported in the table is between –0.06 and 0.05 nm. Thus, the wavelength has not been updated in the Calibration product. It is foreseen not to use the star id 4 for wavelength calibration purposes.

Table 5.3-1: New wavelength assignment calculated for several occultations since November 2002.

Star ID / Level 0 date	1	2	4	9	18	25
20021112_062935	Occ.30: 690.455750	Occ.26: 690.458740		Occ.28: 690.492981		
20021219_102754		Occ.33: 690.468140	Occ.26: 690.875122			
20030101_151630	Occ.3: 690.445068	Occ.37: 690.466003	Occ.30: 690.878540			
20030110_121504		Occ.32: 690.465088	Occ.25: 690.882385			
20030201_090221						Occ.21: 690.492981
20030415_123156			Occ.29: 690.959534		Occ.20: 690.552002	Occ.28: 690.492981
20030419_170041			Occ.29: 690.957520		Occ.23: 690.555420	
20030428_072600					Occ.19: 690.553645	Occ.28: 690. 492981
20030717_053233				Occ. 22: 690.473816	Occ. 26: 690.446594	

5.4 Radiometric Performance

5.4.1 RADIOMETRIC SENSITIVITY

The monitoring performed consists in the calculation of the radiometric sensitivity of each CCD by computing the ratio between parts of the reference spectrum using specific stars. The parts of spectrum used are:

- UV: 250–300 nm
- Yellow: 500–550 nm
- Red: 640–690 nm
- Ir1: 761-770 nm
- Ir2: 935-944 nm

For the spectrometers the ratios are with respect to the 'yellow' spectral range. For the photometers, the ratio is calculated dividing the mean photometer signal above the atmosphere (115 km) by the 'yellow' spectral range (for PH1) or by the 'red' spectral range (for PH2).

The variation of the normalized ratio should be within a given threshold actually set to 10% (see table 5.4-1 that corresponds to fig. 5.4-1). For every star, this variation is calculated as the difference between the maximum (or minimum) ratio, and the mean over the 15 first values (if there are not 15 values computed yet, all values are used). Values outside the warning threshold of 10% are now observed for the photometers, and investigations are on going at ACRI ESL. The star 18 has been studied in depth and two possible causes of these abnormal ratios are in place:

- The pointing azimuth of star 18 is going into the vignetting area during the period of the high peak, so the reference star spectrum used for the computation of the radiometric sensitivity ratio contains a contribution due to the vignetting correction. By looking at the UV and Red ratios of fig. 5.4-1, there is no high variation of the ratio, as the vignetting effect does not affect the SPA. For the IR1 and IR2 ratios the high variation seems to be due to some residual error in the vignetting correction.

- Fig. 5.4-2 shows the difference between the SPA reference star spectra for orbits 08010 (azimuth 17.5 deg) and orbit 08428 (azimuth -9 deg). The shape does not look like a star or the sun spectrum; it rather looks like the reflectivity correction curve. It is known that the reflectivity LUT has to be revised and the ESL is currently working on it.

Whether the vignetting or inaccurate reflectivity correction LUT are responsible for the ratios behavior (maybe both) will be checked in the following months, when there will be an updated of the calibration ADF containing a new reflectivity correction LUT.

Table 5.4-1: Variation of RS for the different ratios. Should be less than 10%.

Star Id	% variation of UV ratio	% variation of Red ratio	% variation of IR1 ratio	% variation of IR2 ratio	% variation of Ph1 ratio	% variation of Ph2 ratio
1	0.543863	0.198668	0.387800	0.193903	4.16760	10.4636
2	0.158766	0.259793	0.418974	0.180858	2.10667	6.07233
4	0.0529779	0.0468850	0.115433	0.233174	2.51800	4.93374
9	1.69204	0.213861	0.364793	0.233455	4.79555	9.05862
18	0.223948	0.167108	0.844914	0.608099	14.7885	299.989
25	2.55773	0.212821	0.225987	0.223921	15.9214	78.6219

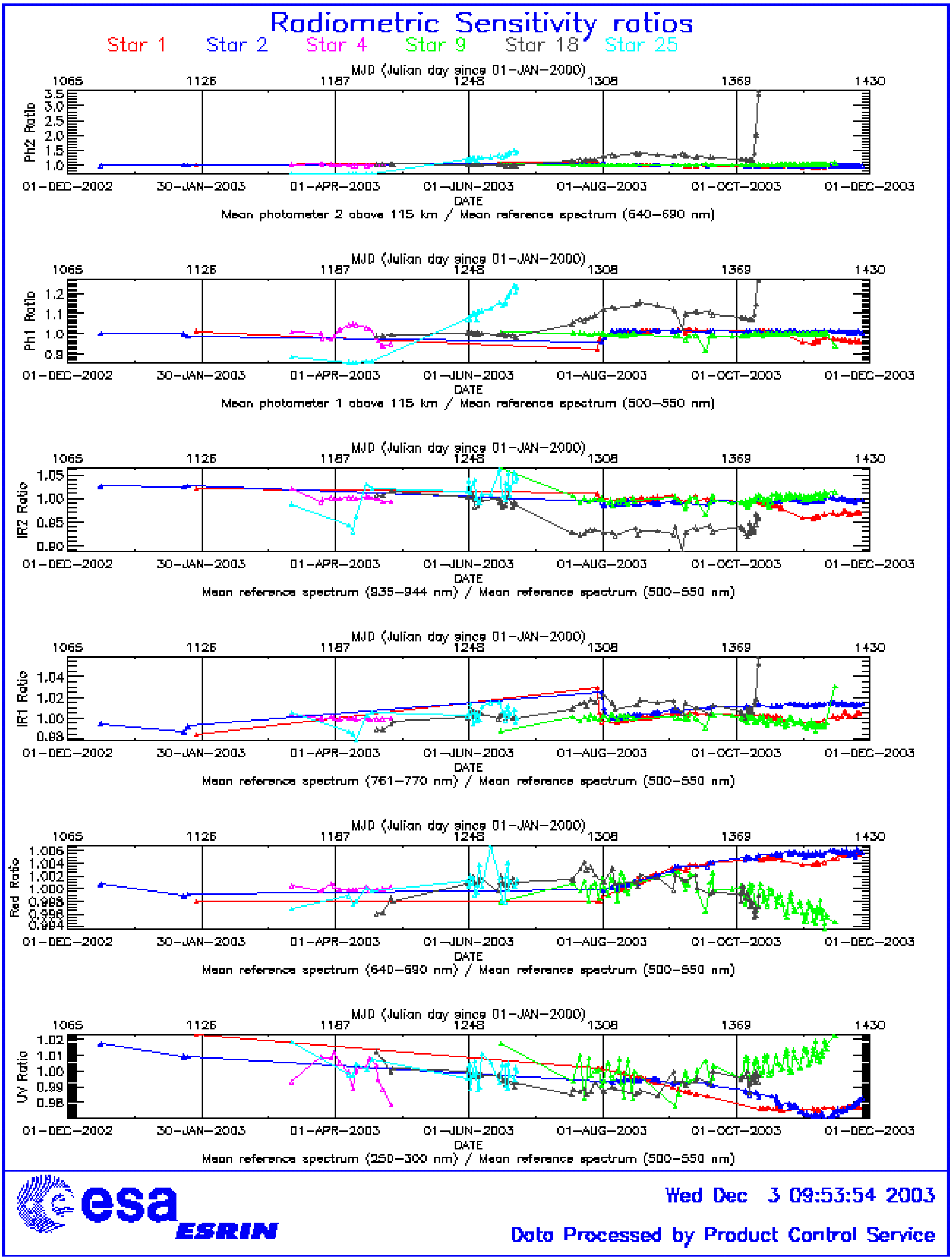

Figure 5.4-1: Radiometric Sensitivity ratios.

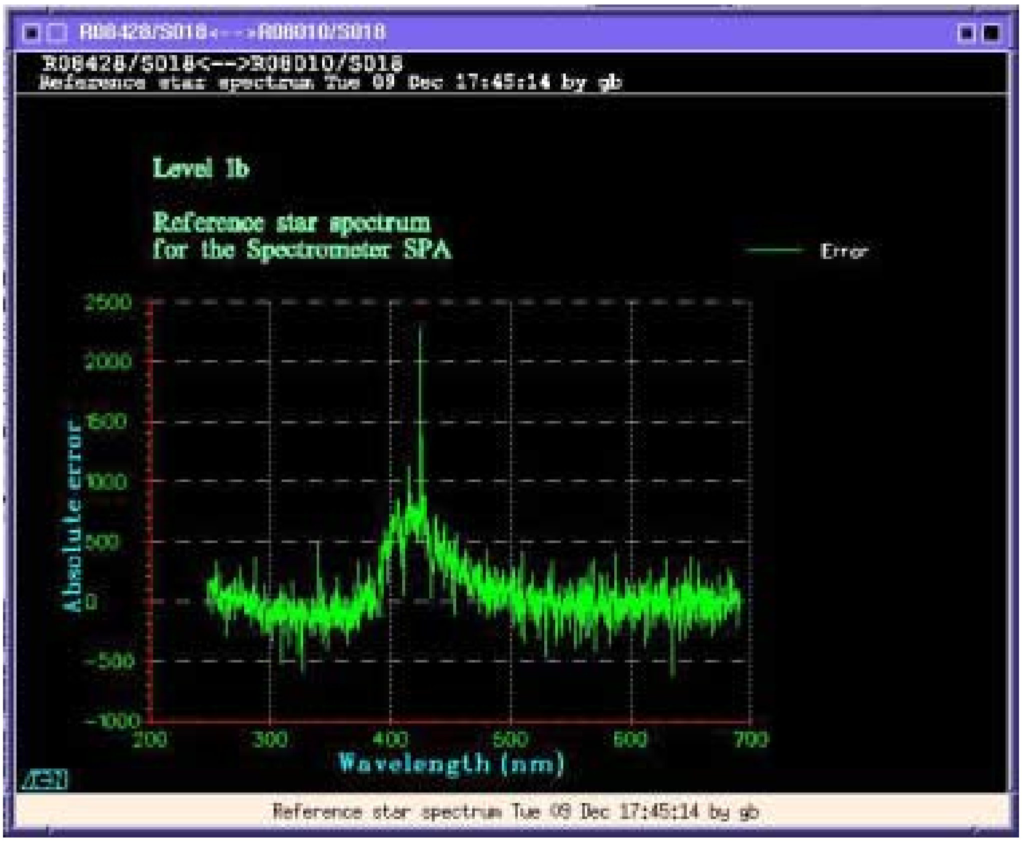

Figure 5.4-2: difference between the SPA reference star spectra for orbits 08010 (azimuth 17.5 deg) and orbit 08428 (azimuth -9 deg)

5.4.2 PIXEL RESPONSE NON UNIFORMITY (PRNU)

No new PRNU calibration has been done during November. During May 2003 a new PRNU calibration has been performed and processed into an update of the PRNU maps for the SPB1 and SPB2 that have been included in the auxiliary file GOM_CAL disseminated at the end of June 2003.

5.5 Other Calibration Results

Future reports will address other calibration results, when available.

6 LEVEL 2 PRODUCT QUALITY MONITORING

6.1 Processor Configuration

6.1.1 VERSION

No level 2 products from the operational ground segment have been disseminated during November to the users. About 80% of GOM_NL__2P products have been received in the PCF for routine quality control and long term trend monitoring. The current level 2-processor software version for the operational ground segment is GOMOS/4.00 (see table 6.1-1) and the product specification is PO-RS-MDA-GS2009_10_3H. The improvements defined at the Validation Workshop are currently being implemented into the prototype processor, before implementation into the operational one. In the mean time, Cal/Val teams are supplied with selected data sets generated by the previous prototype processor GOPR 5.4 (see table 6.1-2).

Table 6.1-1: PDS level 2 product version and main modifications implemented

Date	Version	Description of changes
31-MAY-2003	Level 2 version 4.00 at PDHS-E and PDHS-K	Algorithm baseline level 2 DPM 5.4: • Revision of some default values • Add a new parameter • Transmission model computation: suppress tests on valid pixels and species • Apply a Gaussian filter to the vertical inversion matrix • Very low signal values are substituted by threshold value • See ref. [3] for more details
21-NOV-2002	Level 2 version 3.61 at PDHS-E and PDHS-K	Algorithm baseline level 2 DPM 5.3a: • Revision of some default values • Wording of test T11 • Dilution term computation of jend • Covariance computation scaling applied before and after • See ref. [3] for more details

Table 6.1-2: GOPR level 2 product version and main modifications implemented

Date	Version	Description of changes
18-AUG-2003	GOPR 5.4d	• Tikhonov regularisation is implemented
18-MAR-2003	GOPR 5.4b	• Modification to implement the computation of Tmodel for spectrometer B (in version 5.4b, the Tmodel for SPB is still set to 1)
30-JAN-2003	GOPR 5.4a	• Modifications for ACRI internal use only. No impact on level 2 products.

6.1.2 AUXILIARY DATA FILES (ADF)

The ADF's files in table 6.1-3 and 6.1-4 are used by the PDS to process the data from level 1 to level 2. For every type of file, the validity runs from the start validity time until the start validity time of the following one, but if an ADF file has been disseminated after the start validity time, it is obvious that it will be used by the PDS only after the dissemination time (this happens the majority of the times).

Table 6.1-3: Table of historic GOM_PR2_AX files used by PDS for level 2 products generation

Used by PDS for Level 2 products generation in period	GOM_PR2_AX (GOMOS Processing level 2 configuration file)
01-MAR-2002 → 29-JUL-2002	GOM_PR2_AXVIEC20020121_165624_20020101_000000_20200101_000000 • Pre-launch configuration
30-JUL-2002 → 02-SEP-2002	GOM_PR2_AXVIEC20020729_083851_20020301_000000_20100101_000000 • Maximum value of chi2 before a warning flag is raised (set to 5) • Maximum number of iterations for the main loop (set to 1)
03-SEP-2002 → 12-NOV-2003	GOM_PR2_AXVIEC20020902_151029_20020301_000000_20100101_000000 • Maximum value of chi2 before a warning flag is raised (set to 100)
13-NOV-2003 → today	GOM_PR2_AXVIEC20021112_170458_20020301_000000_20100101_000000 • Smoothing mode • Hanning filter • Number of iterations • Spectral windows to suppress the O2 absorption in the high spectral range of SPA2

Table 6.1-4: Table of historic GOM_CRS_AX files used by PDS for level 2 products generation

Used by PDS for Level 2 products generation in period	GOM_CRS_AX (GOMOS Cross Sections file)
01-MAR-2002 → 08-MAR-2002	GOM_CRS_AXVIEC20020121_164026_20020101_000000_20200101_000000 • Pre-launch configuration
09-MAR-2003 → 29-JUL-2002	GOM_CRS_AXVIEC20020308_185417_20020101_000000_20200101_000000 • Corrected NUM_DSD in MPH - was 14 and is now 19 - and corrected spare DSD format by replacing last spare by carriage returns in file GOM_CRS_AXVIEC20020121_164026_20020101_000000_20200101_000000
30-JUL-2002 → today	GOM_CRS_AXVIEC20020729_082931_20020301_000000_20100101_000000 • O3 cross-sections summary description (SPA) • NO3 cross-sections summary description • O2 transmissions summary description • H2O transmissions summary description • O3 cross sections (SPA)

6.2 Other Level 2 performance issues

The plot presented in fig. 6.2-1 is the average of the Ozone values during November in a grid of 0.5 degrees in latitude per 1 km in altitude. Some characteristics can be seen: part of the ozone hole beyond –60 degrees latitude; the increase of ozone layer thickness at around 20-25 km at high latitudes due to the transport of O_3 rich air masses. However, other characteristics seem not to be realistic (and are under investigation) as the values below 15 km, where data are not reliable at the moment.

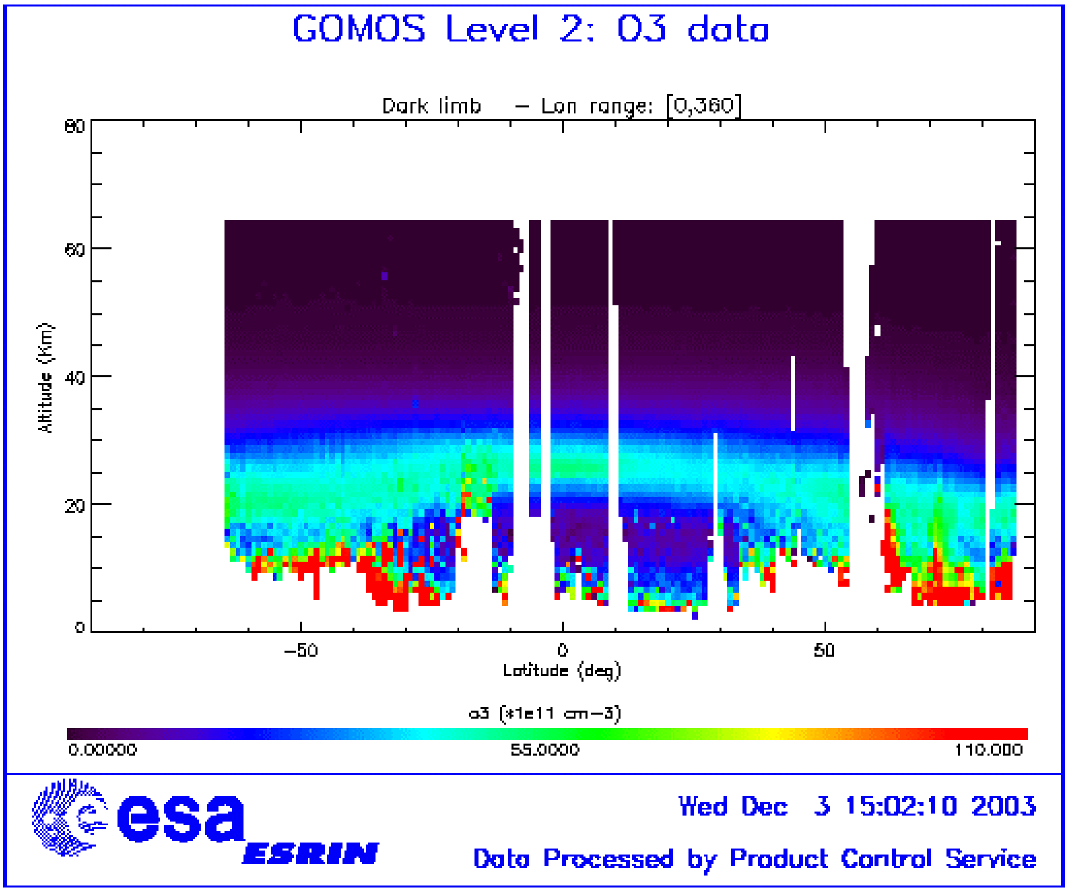

Figure 6.2-1: Average GOMOS O_3 profile during November: average in a grid of 0.5° latitude x 1 Km altitude

7 VALIDATION ACTIVITIES AND RESULTS

7.1 Intercomparison with external data

In this section there are presented comparisons of GOMOS H_2O vertical profiles with HALOE measurements. The conditions of the comparison are as follows:

- GOMOS L2 processing version: v5.4d (including Tikhonov regularisation)
- HALOE processing version: v19; the H_2O concentration profiles are inferred from H_2O mixing ratio profiles using HALOE pressure and temperature vertical profiles.
- The date and position of the measurements, and the distance between GOMOS and HALOE measurement is given on the figures.

For the 6 close coincidences (distance lower than 200km) presented on fig. 7.1-1 to 7.1-6, there is no strong disagreement between GOMOS and HALOE H2O vertical profiles. Nevertheless, in some altitude ranges, GOMOS values are higher than HALOE values: above 30km in fig. 7.1-1; above 25km in fig. 7.1-3; above 20 to 25km in fig. 7.1-4, 7.1-5 and 7.1-6.

For the last two coincidences (fig. 7.1-5 and 7.1-6) GOMOS and HALOE profiles show strong values in the upper troposphere/lower stratosphere.

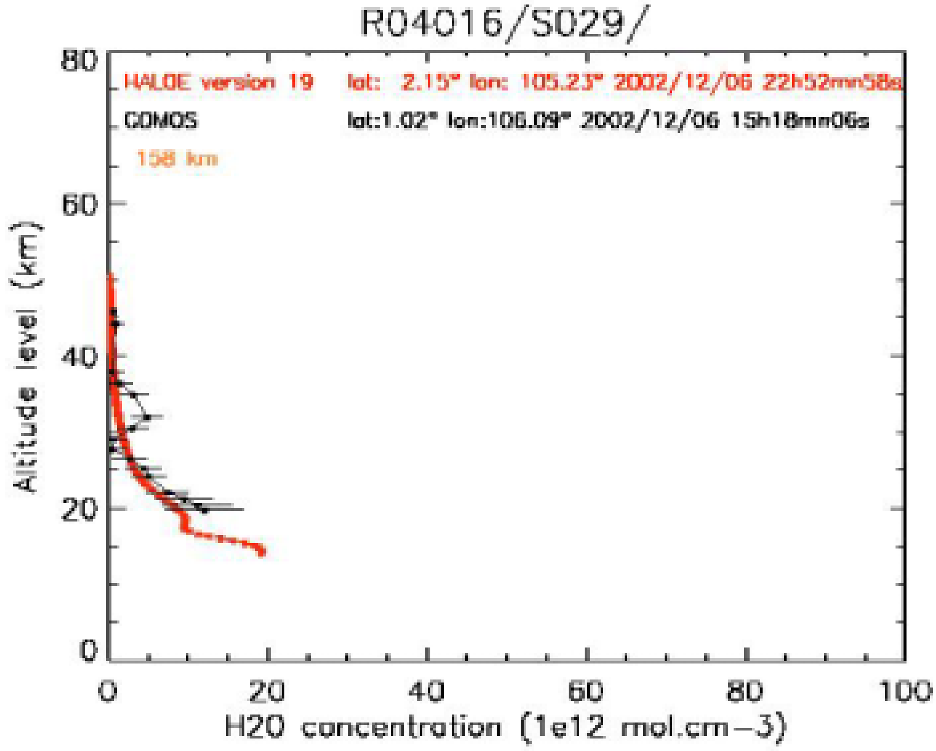

Figure 7.1-1: GOMOS/HALOE H2O vertical profiles. Star # 29 used by GOMOS

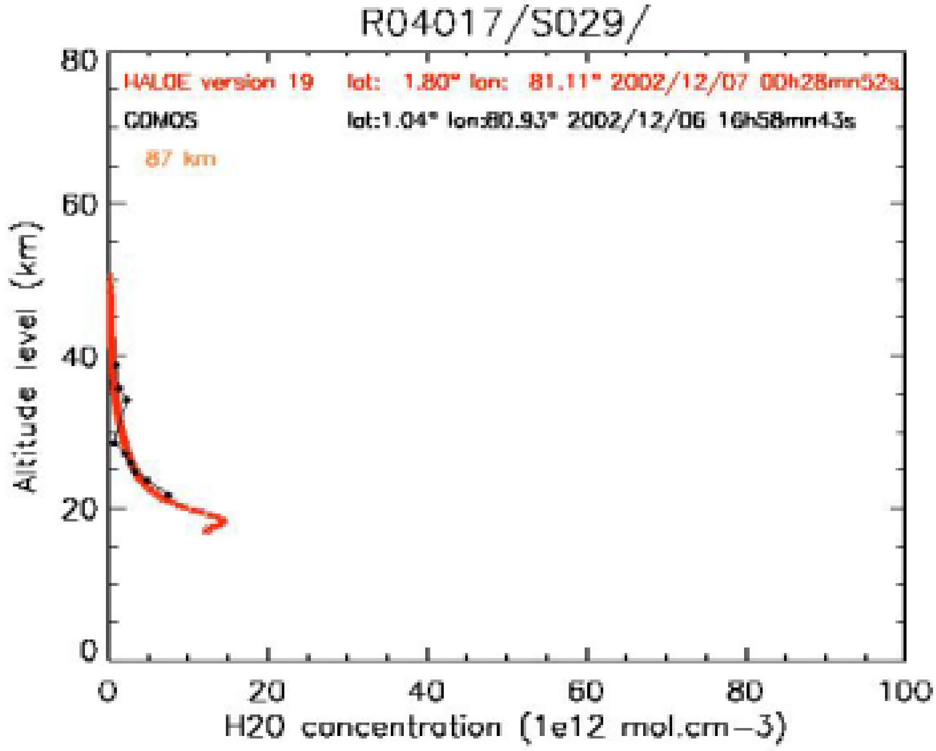

Figure 7.1-2: GOMOS/HALOE H2O vertical profiles. Star # 29 used by GOMOS

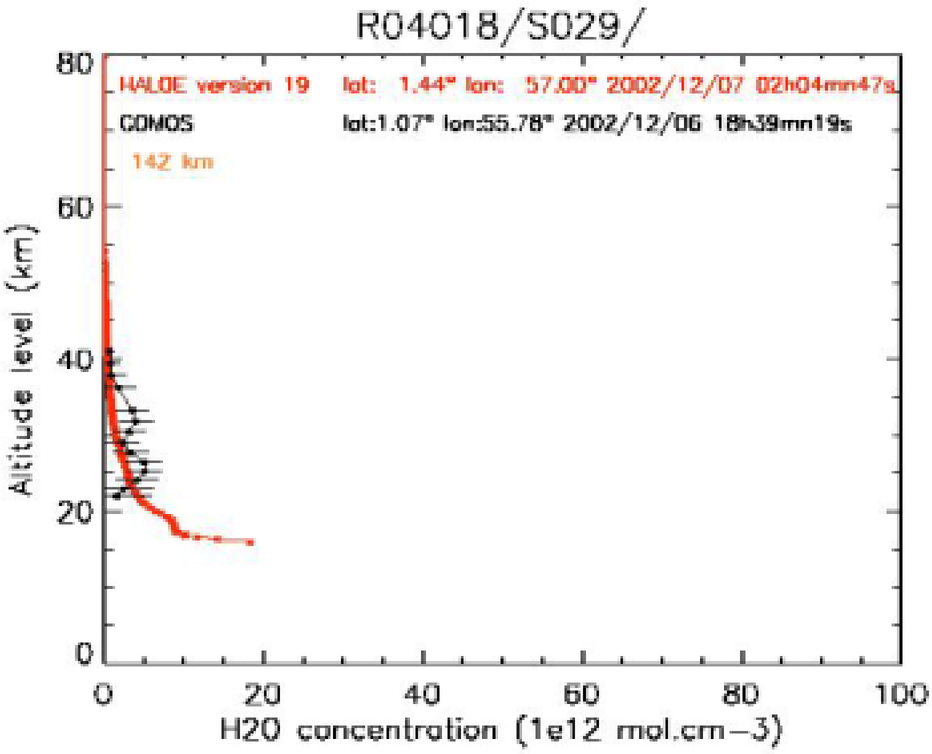

Figure 7.1-3: GOMOS/HALOE H2O vertical profiles. Star # 29 used by GOMOS

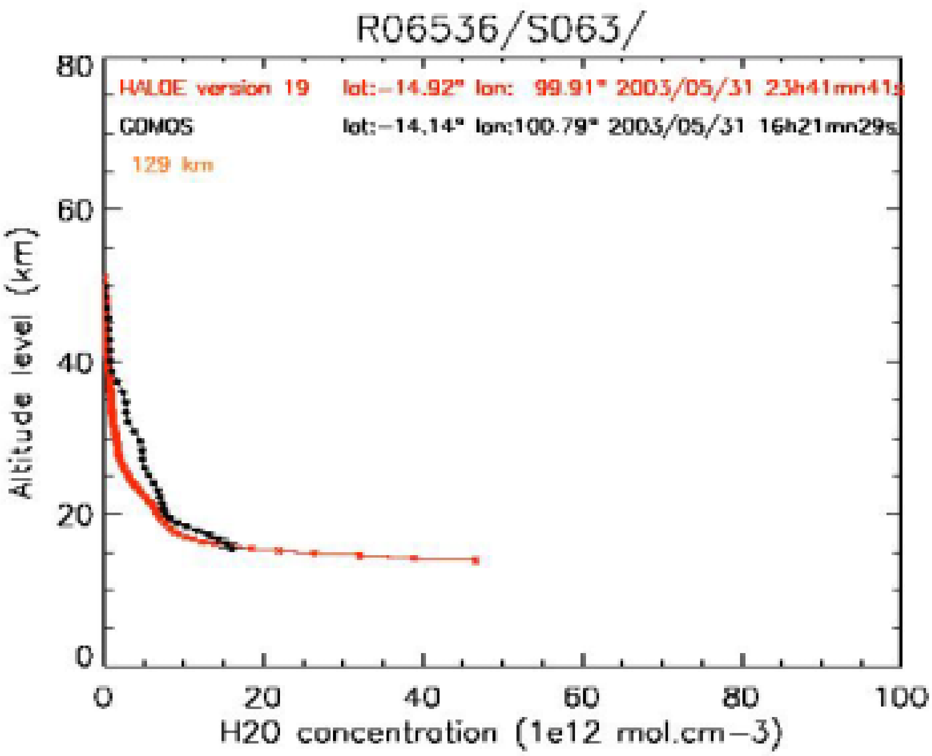

Figure 7.1-4: GOMOS/HALOE H2O vertical profiles. Star # 63 used by GOMOS

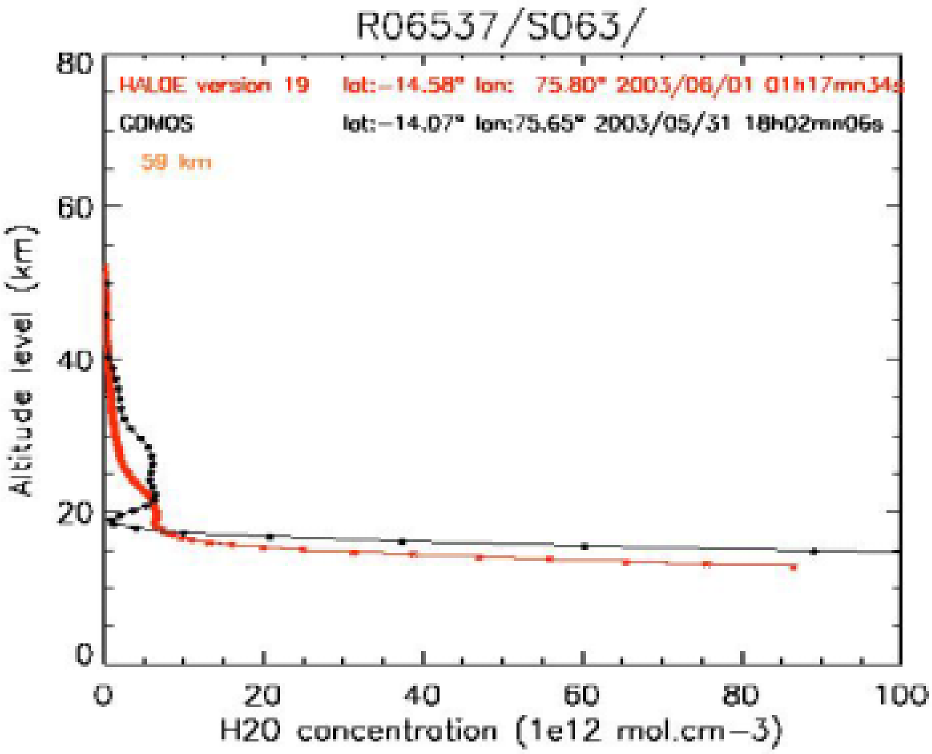

Figure 7.1-5: GOMOS/HALOE H2O vertical profiles. Star # 63 used by GOMOS

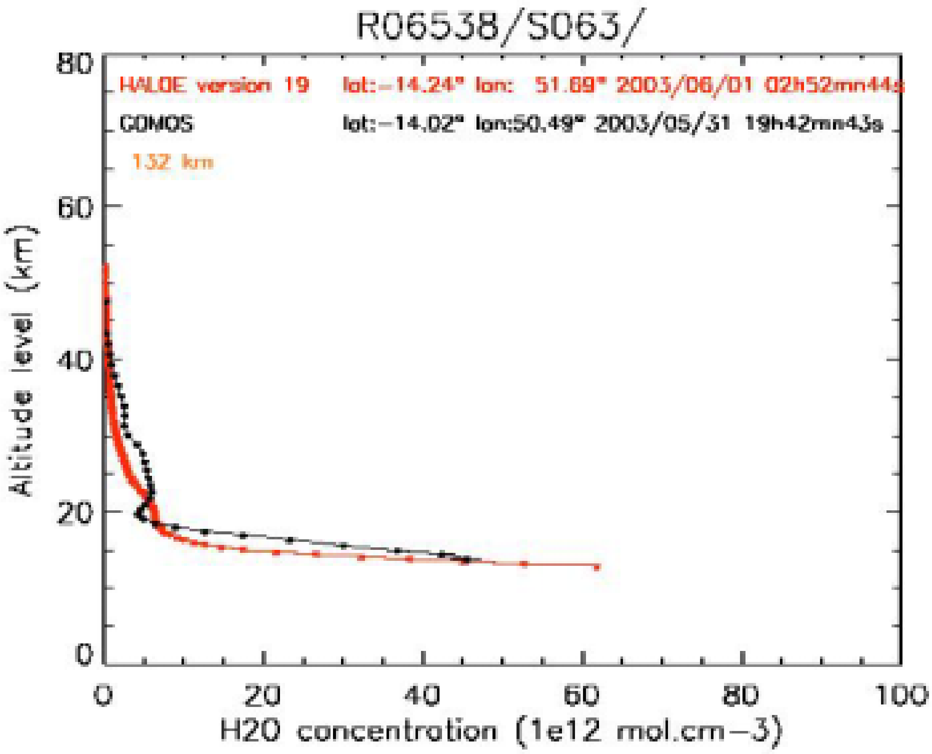

Figure 7.1-6: GOMOS/HALOE H2O vertical profiles. Star # 63 used by GOMOS

7.2 GOMOS-Climatology comparisons

Results will be presented upon availability.

7.3 GOMOS Assimilation

The development of the Antarctic ozone hole in 2003 has been characterized by a rapid growth in August followed by a stable period in September during which the ozone hole exhibits a record size when compared to the previous years. We have attempted to simulate this evolution by assimilating ozone GOMOS measurements in the assimilation system MSDOL. It must be noted, however, that GOMOS does not perform any measurements inside the South polar vortex as illustrated on fig. 7.3-1 that shows the day-by-day location of the GOMOS measurements that have been used for the experiment (only measurements occurring by night are used and flagged data or measurements affected by too large error bars are rejected).

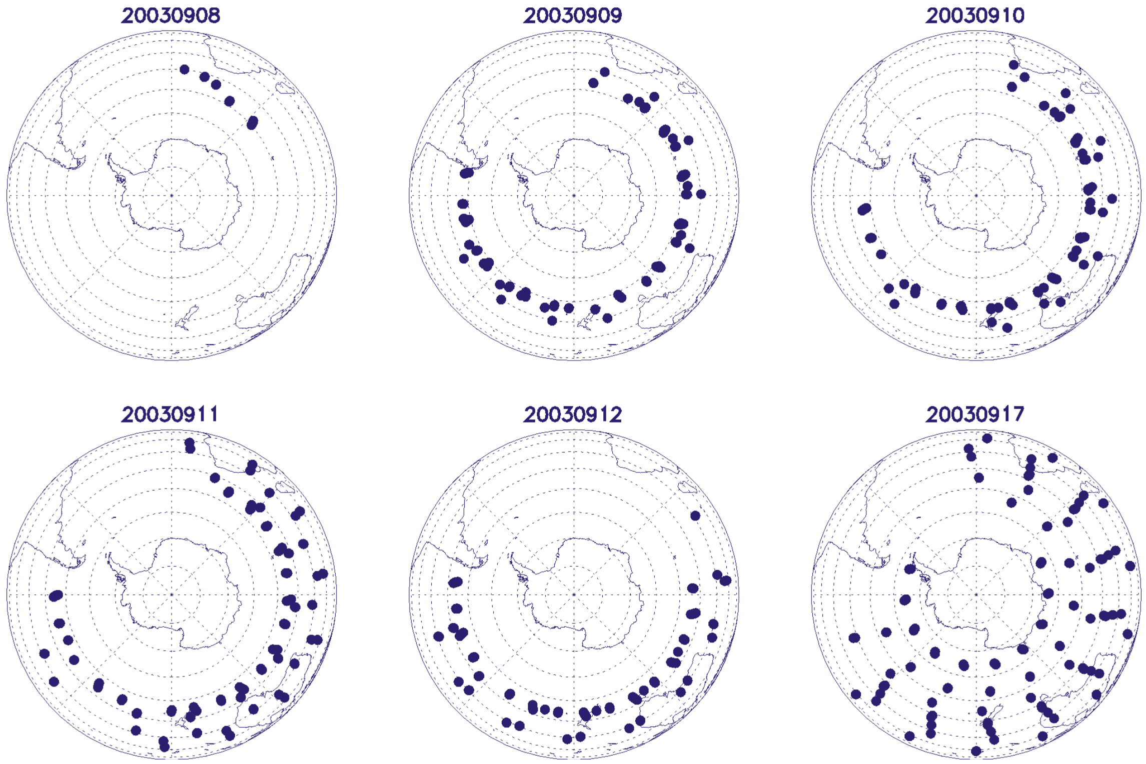

Figure 7.3-1: location of GOMOS measurements used for the assimilation between 08/09/2003 and 17/09/2003

The MSDOL-CTM has been initialized on August 1st 2003 using climatology for all species and run (while assimilating GOMOS ozone measurements) until September 8th. Then two assimilation experiments have been performed from this point: one of them is simply the continuation of the previous run (assimilation of local densities). In the other one, the ozone line densities (integrated along the line of sight) are assimilated. The latter allows bypassing the hypothesis of spherical symmetry that is used when performing the "vertical inversion" from the line to the local densities.

Fig. 7.3-2 shows the time evolution of the ozone field at 66.1 hPa (around 15-20 km altitude that is at the level where ozone destruction is maximum) over Antarctica in September. The swelling of the ozone hole is clearly apparent. In order to assess whether this result provides an accurate view of what has been occurring in reality, a comparison has been performed with the ozone soundings performed from Marambio (on the Antarctic Peninsula) by the FMI, available through the NILU database. The comparison is shown for the level 38 hPa (between 20 and 25 km altitude) on fig. 7.3-3. One can see that the agreement is fairly good during August (MJD2000 between 1308 and 1338) corresponding to the early phase of the development of the ozone hole, when it has not yet reached the latitude of the station. In particular, the peak at the end of August is well captured. On the other hand, the soundings and the values predicted by the model disagree during the first half of September: ozone soundings report ozone depletion that is not observed by on MSDOL results. This can be due to the fact that no (or few) data have been assimilated during that period in the vicinity of the station: indeed, as soon as the assimilation process restarts, the model is driven near low ozone value without reaching the level observed by the soundings, however. It is interesting to note that the results obtained by assimilating line densities seem in a slightly better agreement than the ones obtained by assimilated local densities. This however may be the effect of the error estimation put on the measured values.

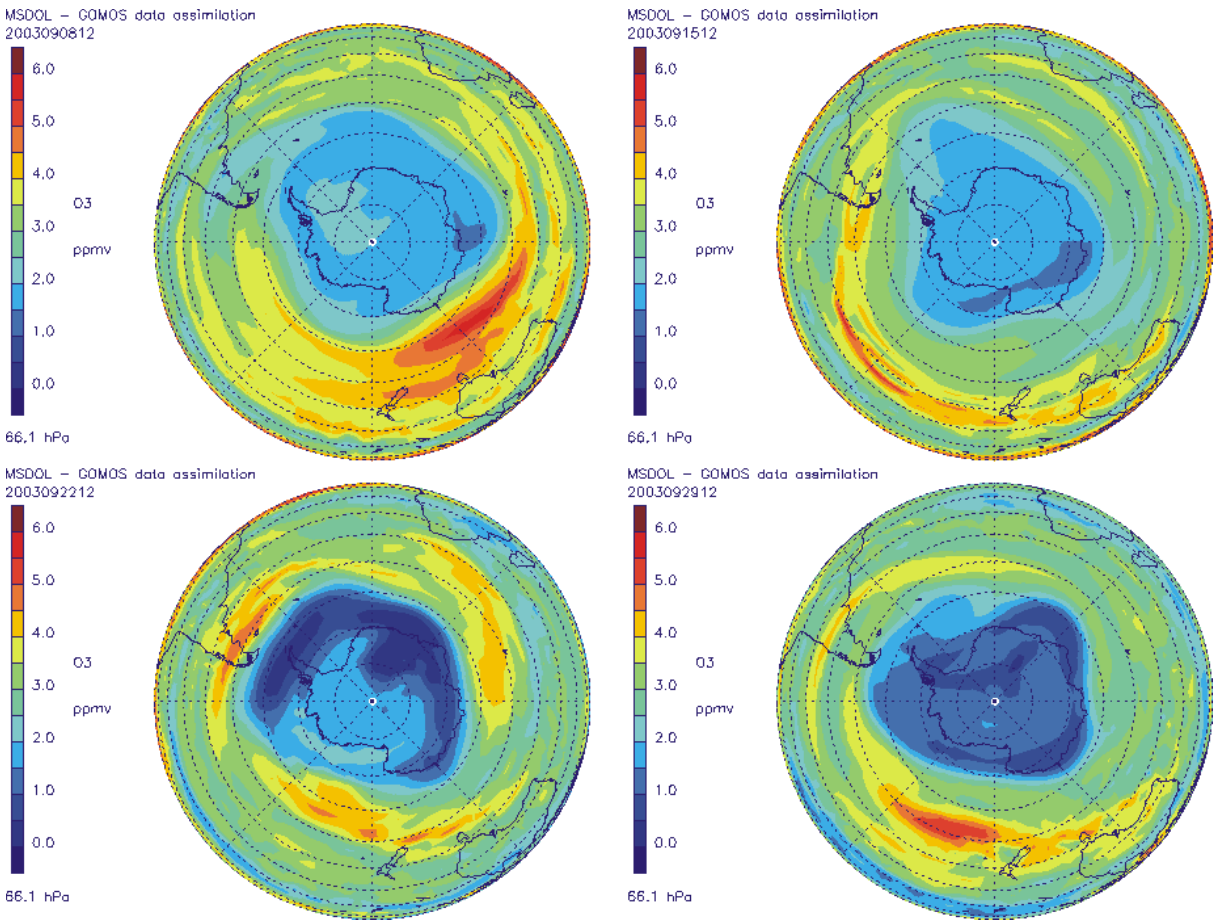

Figure 7.3-2: Time evolution of the ozone field at 66.1 hPa (around 15-20 km altitude) over Antarctica for four dates in September 2003

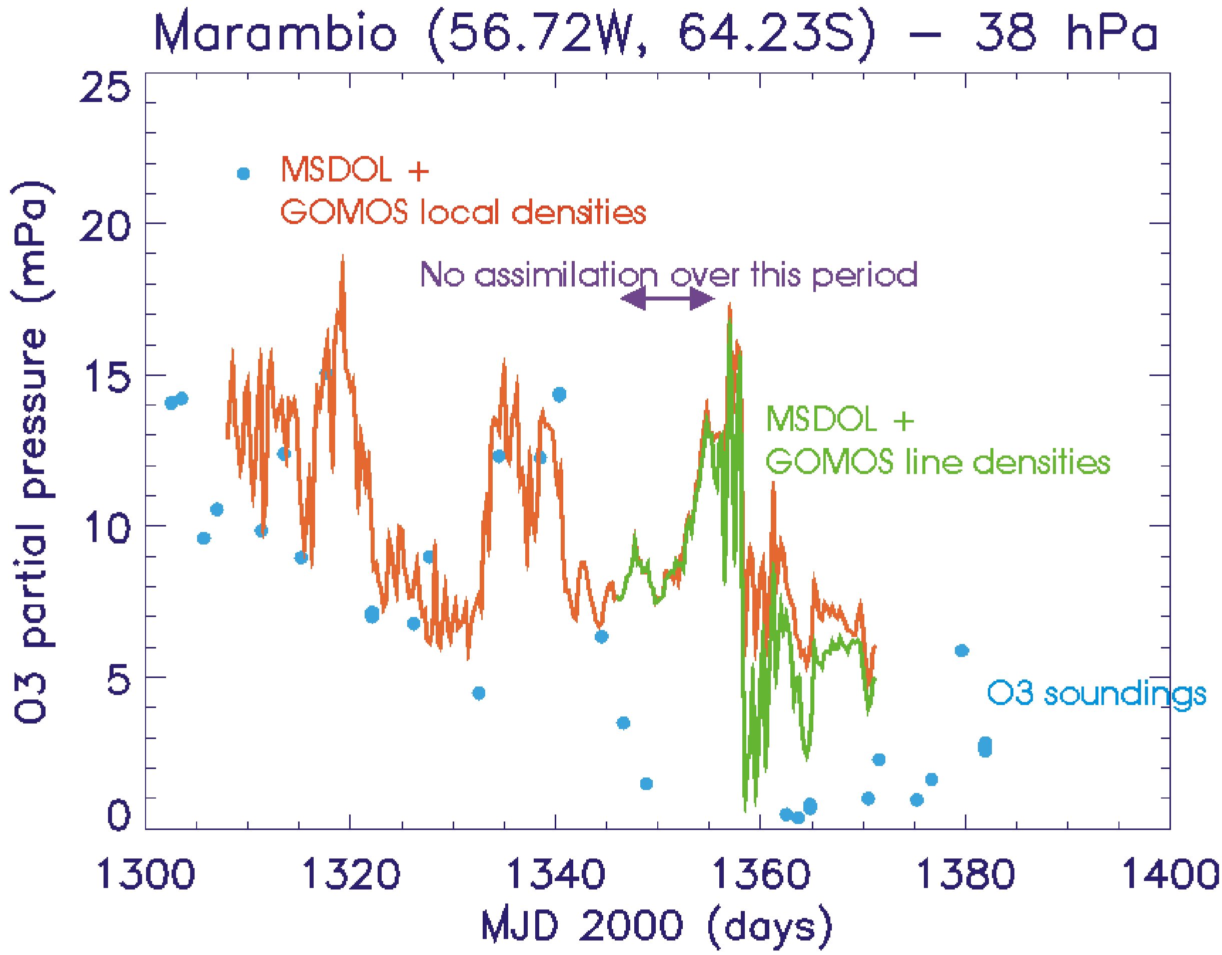

Figure 7.3-3: Time evolution of the ozone pressure at 38hPa (between 20 and 25 km altitude) at Marambio (on the Antarctic Peninsula) inferred from two MSDOL runs and measured by ozone soundings. The ozone soundings are operated by the FMI and are available through the NILU database

7.4 Consistency Verification: GOMOS-GOMOS intercomparison

Results will be presented upon availability.